

1979

A feasibility study on the use of sandwich construction in prebuckled arches

David Nelsen
Iowa State University

Follow this and additional works at: <https://lib.dr.iastate.edu/rtd>

 Part of the [Civil Engineering Commons](#)

Recommended Citation

Nelsen, David, "A feasibility study on the use of sandwich construction in prebuckled arches" (1979). *Retrospective Theses and Dissertations*. 17286.

<https://lib.dr.iastate.edu/rtd/17286>

This Thesis is brought to you for free and open access by the Iowa State University Capstones, Theses and Dissertations at Iowa State University Digital Repository. It has been accepted for inclusion in Retrospective Theses and Dissertations by an authorized administrator of Iowa State University Digital Repository. For more information, please contact digirep@iastate.edu.

CE 690

A FEASIBILITY STUDY ON THE USE OF
SANDWICH CONSTRUCTION IN PREBUCKLED ARCHES

Submitted to
Amdé M. Wolde-Tinsae
Assistant Professor, Department of Civil Engineering
Iowa State University

by
David Nelsen

September 1979

TABLE OF CONTENTS

	<u>Page</u>
1. INTRODUCTION	1
2. SPECIMEN DESCRIPTION	3
3. TEST APPARATUS	9
3.1 General Setup	9
3.2 Loading Mechanism	9
3.3 Data Recording Instrumentation	13
3.4 Test Procedures	14
4. TEST RESULTS	15
4.1 Arch Test Results	15
4.1.1 Model TP I	15
4.1.2 Model TB I	20
4.1.3 Model TO I	27
4.1.4 Model TO II	35
4.1.5 Model TO III	36
4.2 Shear Test Results	46
EVALUATION OF RESULTS	59
5.1 Arch Results	59
5.2 Shear Specimen Results	61
SUMMARY AND CONCLUSIONS	63
REFERENCES	65
APPENDIX A	67
APPENDIX B	68

1. INTRODUCTION

Designers have often turned to sandwich construction¹ when the strength to weight ratio has been an important design consideration, as in the aerospace industry. This research is part of an on-going feasibility study of a new type of structural system termed the "prebuckled dome" by Wolde-Tinsae (1,2). The primary objective of this research is to investigate the feasibility of using a special type of sandwich construction to form the skeleton of this system. For experimentation purposes, five tests were performed. The procedures used and the results will be presented herein.

Prebuckled dome construction involves the buckling of shallow flat members, which are initially straight, into the shape of an arch and their assemblage into a dome. The prebuckled sandwich arch is formed by laminating the core material to one face of the sandwich panel and buckling it into shape. The other facing is then buckled into shape and laminated to the core thus forming the composite section. For this investigation, a discrete core will be used composed of blocks of wood spaced at various intervals.

There are numerous possible applications for this type of structural system. One such example is for use in a long span structure, such as a stadium enclosure. In this type of structure, its own dead weight plays an important role. It was reported by Kennedy and Agarwal that for longer arches, arch weight has "a more pronounced effect on buckling loads"(3). Another area where a high strength to weight ratio is of importance is in the area of seismic design. Here, structural mass translates into force, therefore, in general, the lighter the structure, the less force which is developed.

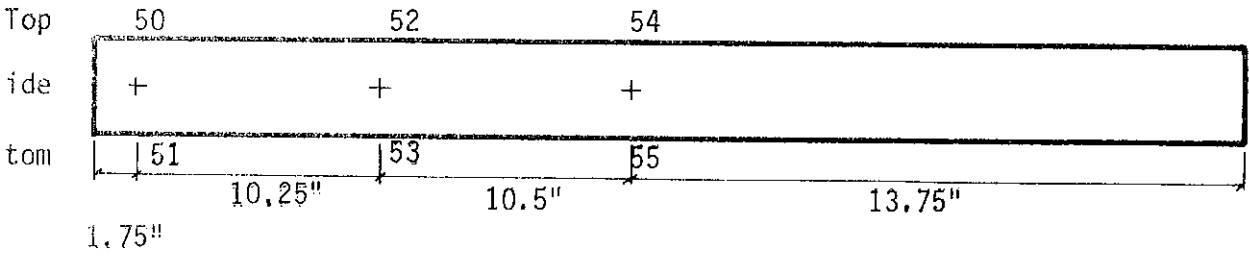
1. In this paper, sandwich construction will be defined as, a layered construction formed by bonding two thin facings to a core material, resulting in composite action between the two.

In addition to the primary objective as stated above, secondary objectives of this research include determining various characteristics of the prebuckled sandwich arch such as maximum load and failure modes. To this end, five models were constructed. The first model had no core and was used as a basis for comparison of the remaining four models. To limit the scope of this research, in the remaining four models, variations of only one type of discrete core were used in an attempt to isolate various failure modes.

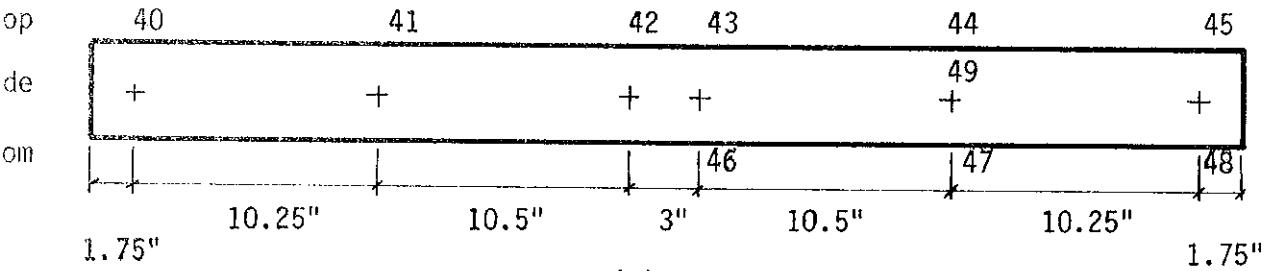
2. SPECIMEN DESCRIPTION

The first model (TPI), which was used as a basis for comparing the rest of the models, was constructed from a piece of 2024 T3 aluminum .040 inch thick, three inches wide and 48 inches long. This thickness was chosen because it is twice as thick as each sandwich facing, thus suggesting the characteristics of an arch with no core. Figure 1a shows the location of the strain gages which were mounted on this model for testing. The arch was then buckled into shape and mounted on hinges that were attached to the testing platform. The model was then ready for testing.

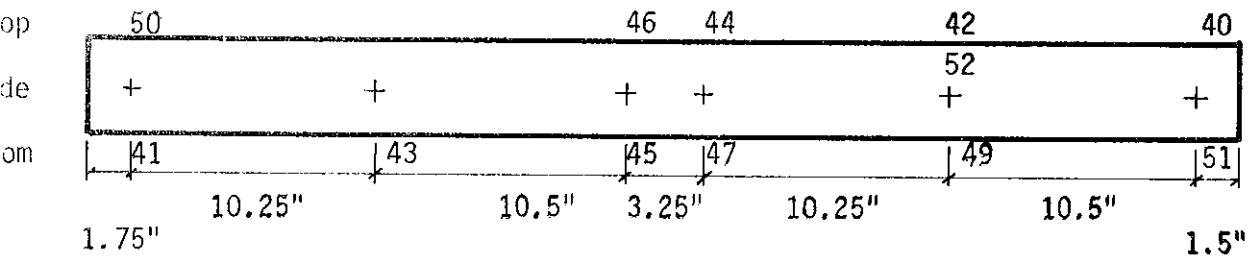
The remaining four models utilized sandwich construction with two types of wood at different spacings. Construction of these arches was complicated by the fact that the arch members could not be manufactured in the flat configuration and then buckled into shape as the first model had been, due to the rigidity exhibited by sandwich construction. Standard sandwich construction uses the facings of the panel to account for most of the bending and in plane rigidity. The core acts compositely with the facings, preventing one facing from sliding with respect to the other and increasing their distance from the neutral axis, much the same as the web of an I beam. To prevent this composite action during the erection procedure, the core was initially laminated to only one facing. It was decided to make the initial lamination to the bottom facing, so that final lamination would be made on the top surface, thereby preventing overhead work. After the wood core was laminated to the bottom face, the adhesive was allowed to cure. The heat curing process used for the AE 15 adhesive is shown in Figure 2a. After curing, the top face and bottom face, with core attached, were buckled into shape. Adhesive was applied to the top face and the panel was clamped and allowed to cure as shown in Figure 2b. The AE 15 adhesive used requires



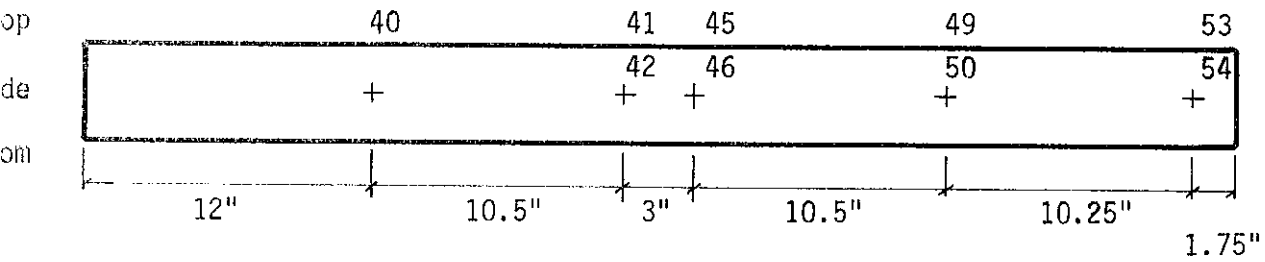
(a)



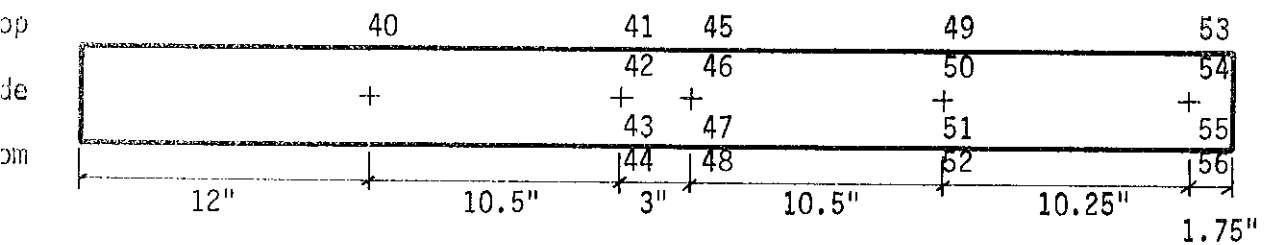
(b)



(c)

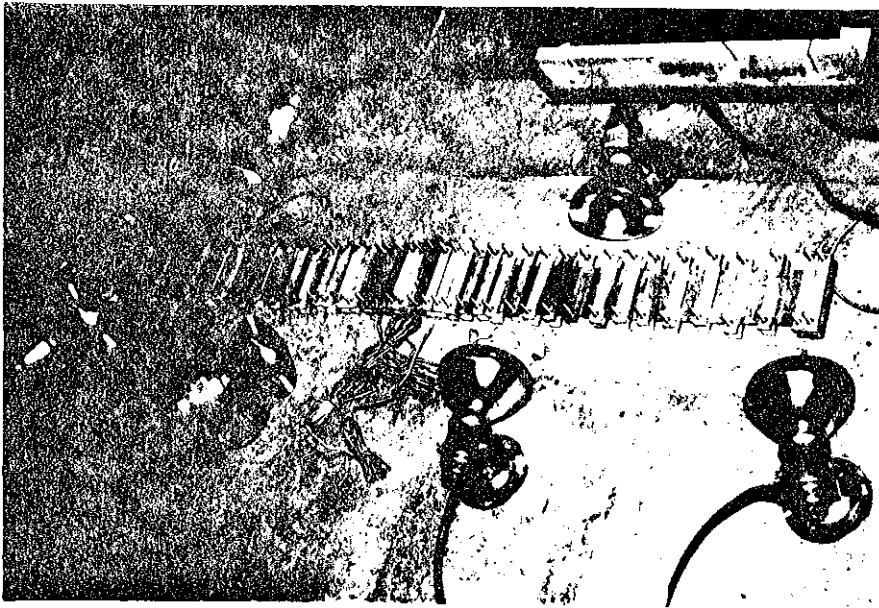


(d)

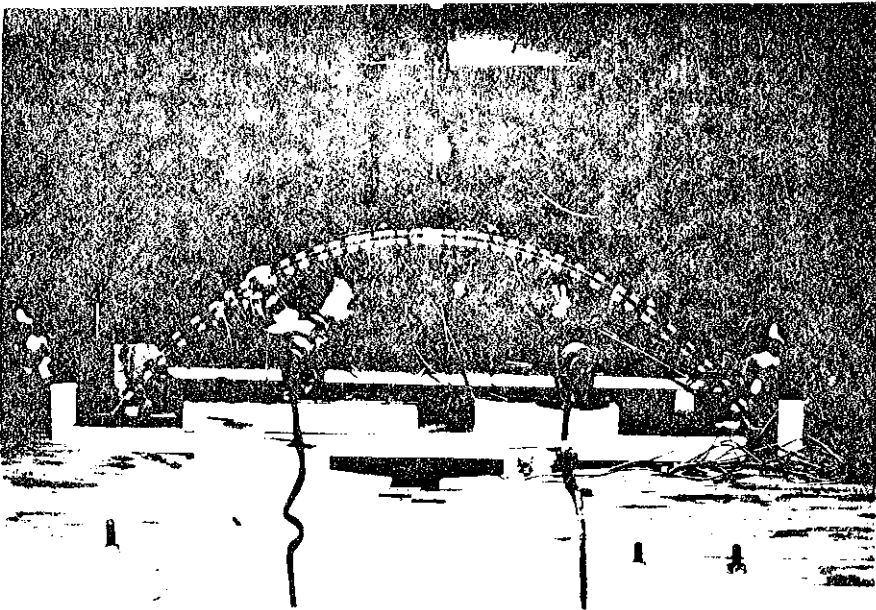


(e)

Strain Gage Locations
Figure 1



(a)



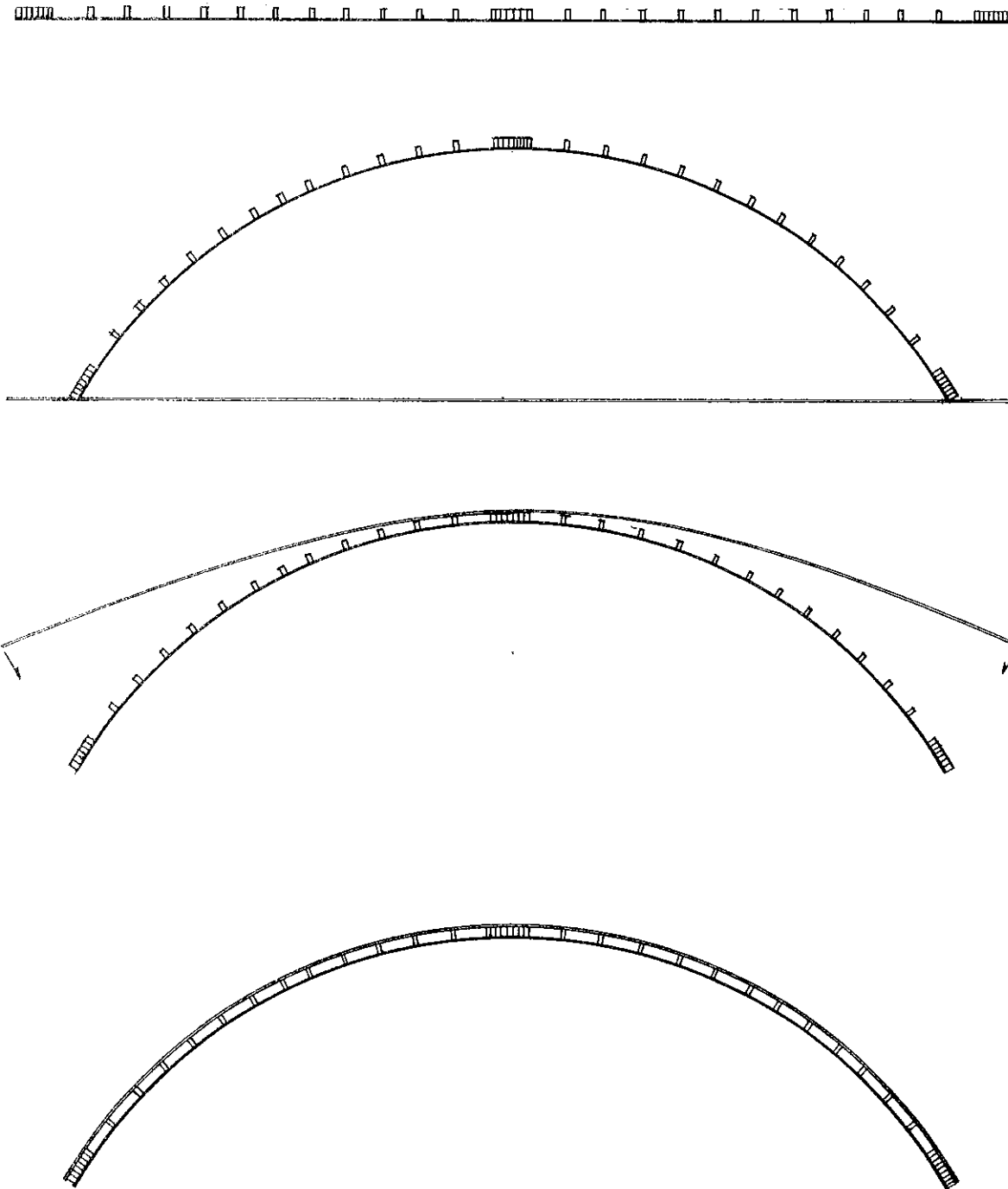
(b)

Figure 2

six hours of curing time at 70 degrees C. The erection procedure is shown schematically in Figure 3. Once the adhesive cured, the composite action typical of sandwich construction took over, locking the arch into the buckled shape. At this point, it was noted that even upon removing the arch from its supports, there were no visible indications of any attempt by the arch to rebound to its flat configuration.

For the models involving sandwich construction adhesive was used for lamination in all cases except for test T0 III, in which the adhesive in conjunction with bolts was used. The facing material used in all of the sandwich arches was 2024 T3 aluminum, .020 inch thick. A discrete core was constructed with balsa wood in test TB I and oak in tests T0 I, T0 II and T0 III and spaced at various intervals. Table 1 gives a summary of materials used for the core and the facing, as well as the spacings used for the different tests. Figures 1b,c,d and e give the strain gage locations used in tests TB I, T0 I, T0 II and T0 III respectively.

In sandwich construction special consideration must be given to details at locations where loads or restraints are applied. For the models tested in the laboratory, special closure clamps were made for the ends of the arch which were then attached to the hinges. The end clamps facilitate the transfer and distribution of restraint loads. Where these clamps attach to the sandwich arch, the core was spaced at much closer intervals to relieve the stress concentrations resulting at these locations. At the center, where the load was to be applied, the core was also spaced at much closer intervals to alleviate stress concentrations and also to prevent local buckling due to the application of the load.



Erection Procedure
Figure 3

SPECIMEN LIST

Test	Facing	Core	Adhesive	Core Spacing	Variations
TP1	.040 2024T3 Aluminum	None	None	None	
TB1	.020 2024T3 Aluminum	Balsa	Commercial Epoxy (Scotch)	.625" O.C.	
T01	.020 2024T3 Aluminum	Oak	AE15	1.875" O.C.	
T0II	.020 2024T3 Aluminum	Oak	AE15	Linear*	*Span 1 .625" center to center following spans increase by .0625".
T0III	.020 2024T3 Aluminum	Oak	AE15	Linear*	*Each core element bolted at same spacing as T0II.

Table 1

3. TEST APPARATUS

3.1 General Setup

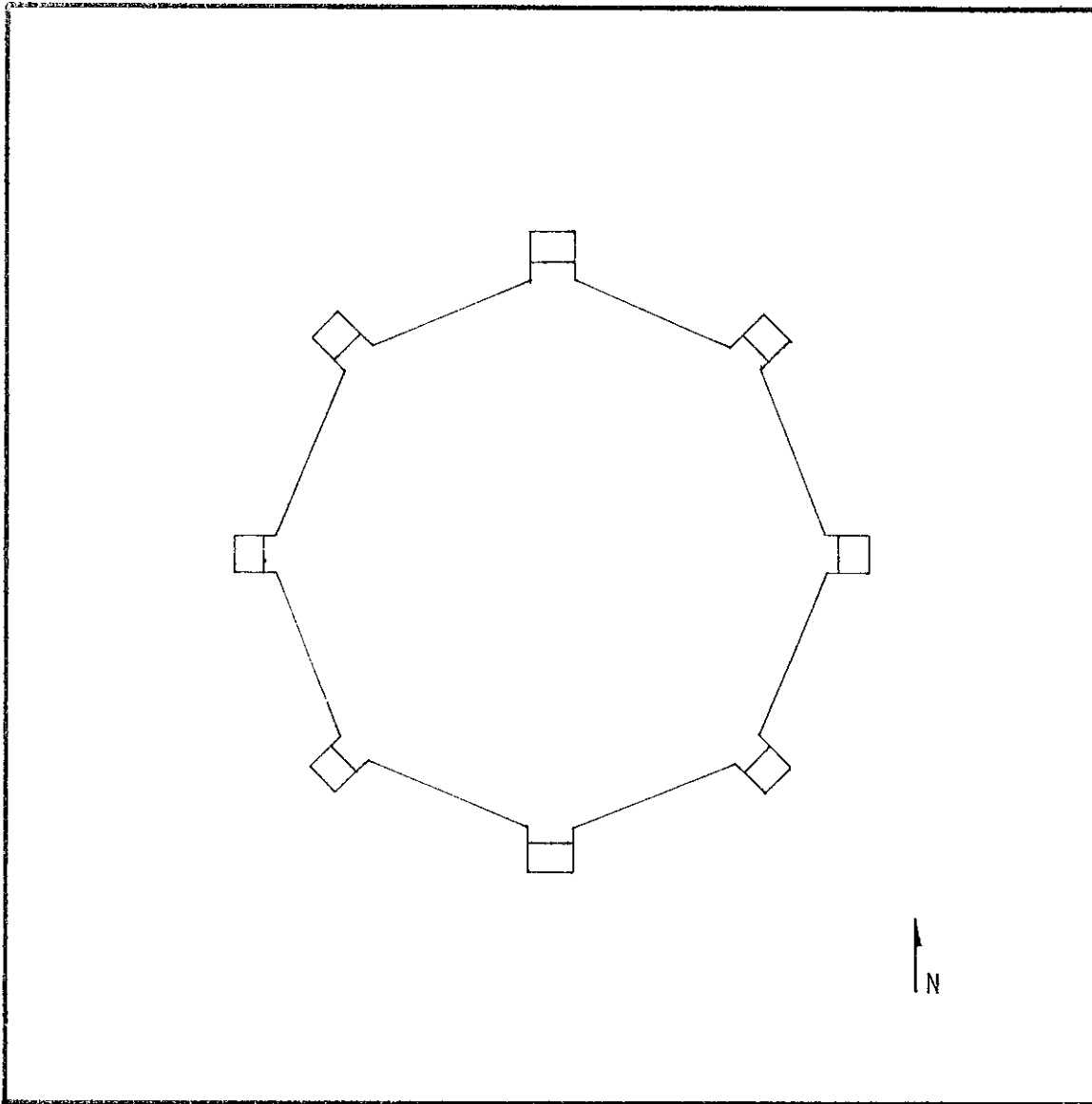
A six foot square plywood platform was constructed on an existing frame in the laboratory for the purpose of testing the arches. The platform was supported on two sides by I beams, which were part of the frame. This platform was one which had been used in earlier testing of the prebuckled dome and was modified for use in the testing of the arches (Figure 4). An opening in the platform allowed for the crown of the arch to be taken lower than the supports. The supports for the arch consisted of hinges, which were located at the edge of the opening. This allowed for rotation at the support, but at the same time restricted horizontal and vertical displacement.

The load was applied by controlling the displacement of a threaded rod, which had a loading mechanism attached to its end. This rod passed through a hole in a steel plate, which was secured to two channels, part of the existing frame, above the model. The height of the rod was controlled by turning a nut which had been threaded onto the rod. The rod was prevented from turning by a stabilizing mechanism as shown in Figure 5. Also shown in Figure 5 is the overall test setup.

3.2 Loading Mechanism

The loading mechanism shown in Figure 6 consists of a load cell, which was attached to a ball joint. Attached to the other side of the ball joint was a four inch aluminum bar which had been cut in half to serve as a loading bar. This allowed for the uniform application of a line load across the top of the arch. Two 1/16 inch rods were placed in the loading bar such that they would pass through holes drilled in the crown of the arch and into a loading bar that was tightened against the bottom of the arch. Upon tightening this loading

A



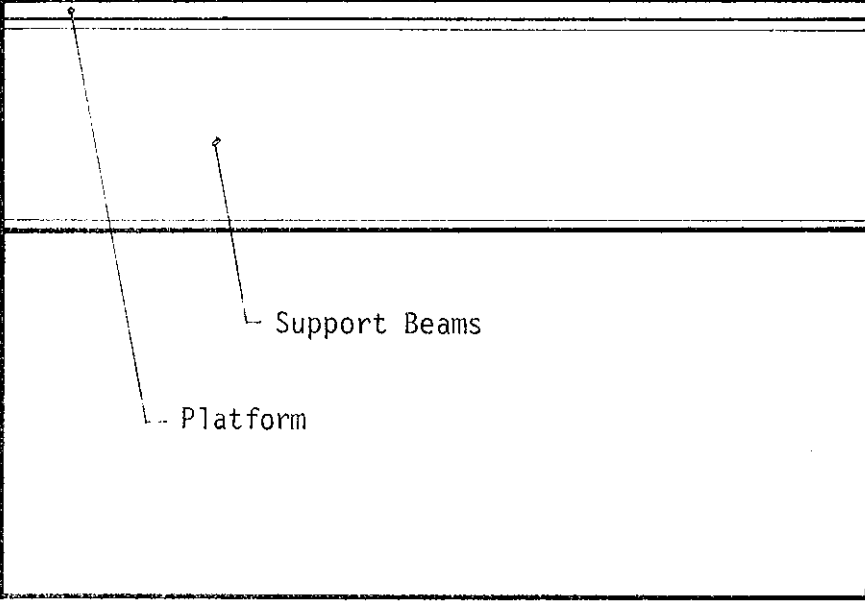
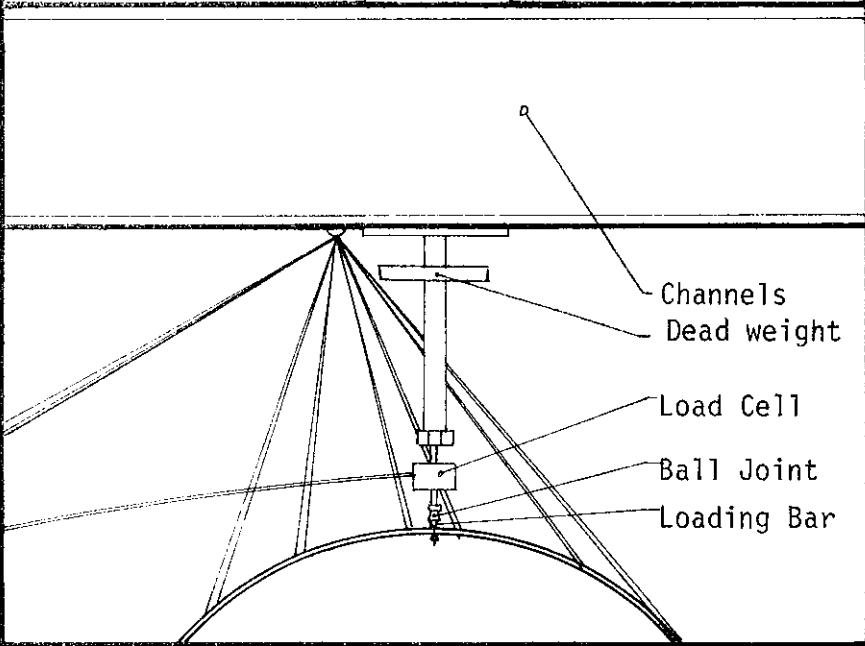
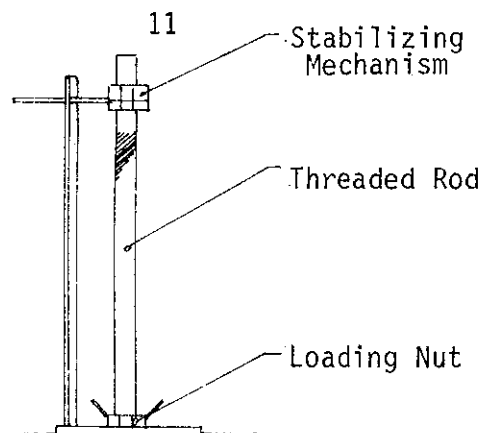
A



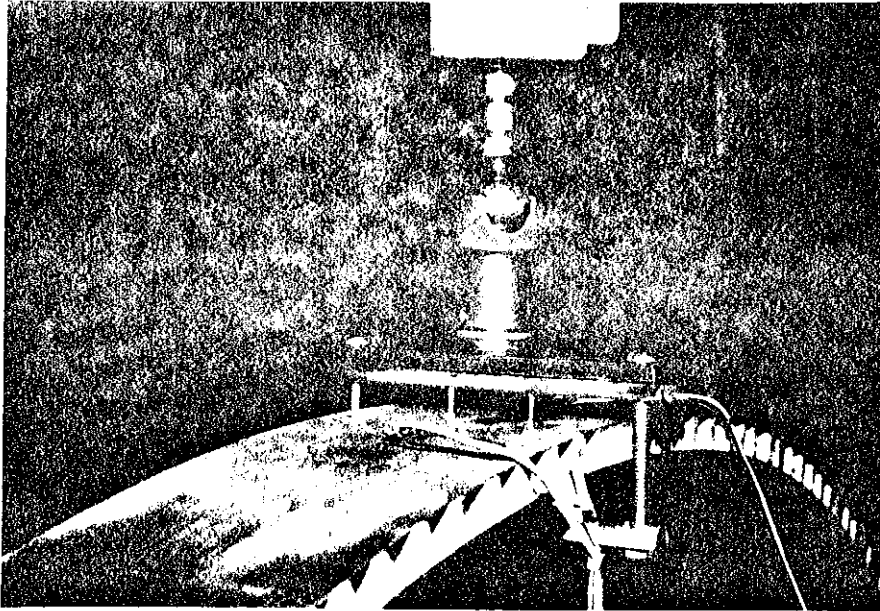
Section A-A

Testing Platform

Figure 4

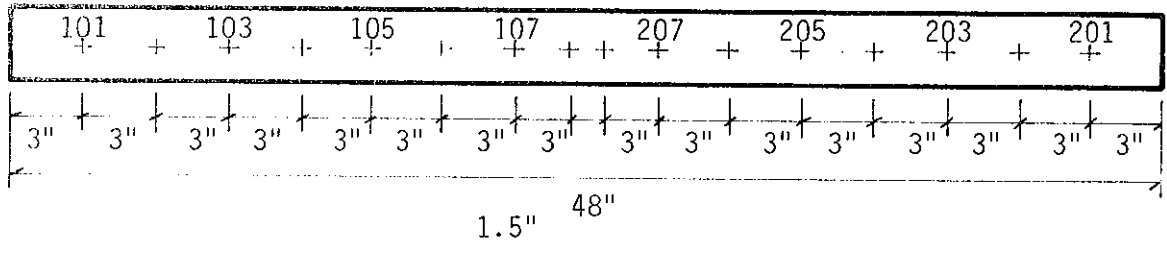


Test Setup
Figure 5



Loading Mechanism

Figure 6



Target Location

Figure 7

plate, the crown of the arch was fixed against horizontal displacement. This was done to eliminate unsymmetric failure, which would require a much more complicated loading mechanism capable of translation along the length of the arch.

3.3 Data Recording Instrumentation

The instrumentation used in testing the arches was devised to measure three different quantities; the applied load, strains on various surfaces and the in plane displacements.

The load cell mentioned previously was a JP1000 load cell having a load capacity of 1000 pounds. Prior to testing the load cell was calibrated and a calibration curve is presented in Figure A1 of the appendix.

Strain gages were used to record the surface strains at various locations on the different models tested. The type of strain gages used were EA-13-125BB-120 from Micro-Measurement. The gages have a gage factor of $2.10 \pm .5\%$. The various gage locations will be found in the individual discussions of each test. The load cell and strain gage readings were recovered using a data acquisition system (Digitrend 210) at various displacement increments throughout the test.

In plane displacement measurements were not of primary interest in these tests and thus only crude measurements, accurate to $1/32$ inch were taken as supplemental information. These measurements were taken from a fixed plane above the model and referenced to the level of the platform. Targets indicating points to be measured were located every three inches along the leg of the arch. An additional target was located at $3/4$ inch on either side of crowns. Figure 7 shows target location while the arch was in the flat configuration. To provide a record of each test, photographs were taken

at various intervals, including curing and testing.

3.4 Test Procedures

The tests were conducted as follows; after allowing the instrumentation the proper amount of time to warm up, readings were taken while the arch was in the flat configuration. The arch was then buckled into shape and another reading taken. Finally, the arch was laminated and clamped for curing. Another reading was taken here completing the erection portion of the test. After the proper cure time, the tests were ready to begin. Another reading was taken and called load point zero. The test then proceeded, stopping at various displacement increments to record load cell and strain gage readings, in plane displacement readings when desired, and to take photographs.

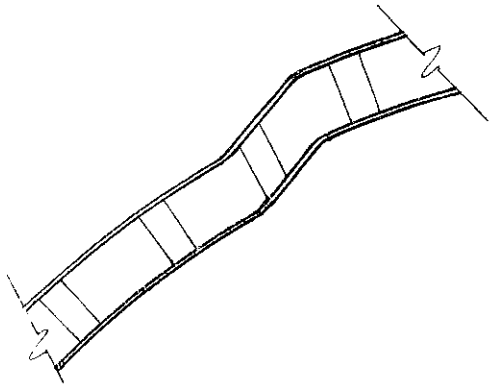
4. TEST RESULTS

4.1 Arch Test Results

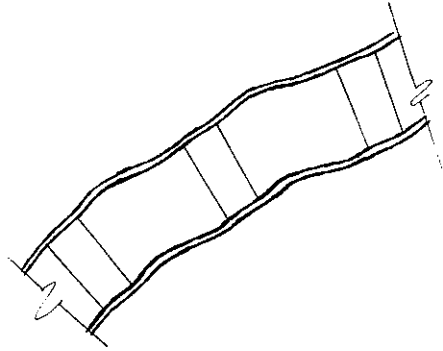
A general discussion of each of the five tests will be presented herein. Observations from each test, as well as behavior exhibited and possible failure modes for each specimen will be included in this discussion. The spans and blocks referred to in each test will be located as shown in Figure 9. Most of the results will be presented in the form of graphs showing load versus displacement or load versus strain. A complete listing of the data obtained from each test is given in Appendix B.

4.1.1 Model TP I

Test TP I was performed to determine the load carrying capacity and resulting strains in an arch with no core. As shown in Table 1, 2024 T3 aluminum .040 inch thick was used to construct the model. Strain readings of the arch were taken while flat and again after it was buckled and pinned to the testing platform. The load cell was then lowered into position and connected to the arch (Figure 10a). Readings were again taken with zero load on the arch and this was called load point zero. Figure 11 shows the initial pre-strain recorded by strain gages at load point zero. As the test was performed, the arch behaved symmetrically (Figure 10b) until the south leg snapped through after load point 20. At that time there was an abrupt change in the load-deflection curve (Figure 12) as well as the load-strain curves (Figure 11). Due to the flexibility of the aluminum, the arch was able to undergo large scale deflection (5.75 inches) before reaching its peak load and even much larger deformation (17.625 inches) before the north leg snapped through. At load point 20 the crown of the arch was actually 5.75 inches below the platform height before the leg of the arch snapped through. The maximum load attained in



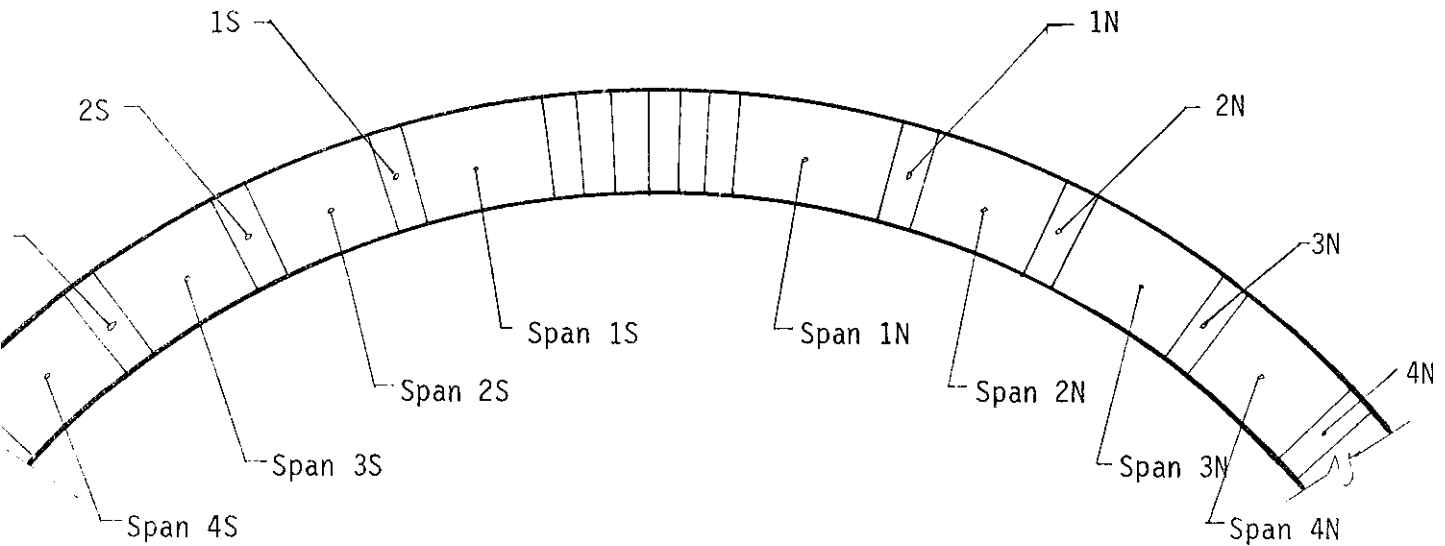
(a) Shear Crimp



(b) Intercellular Buckling

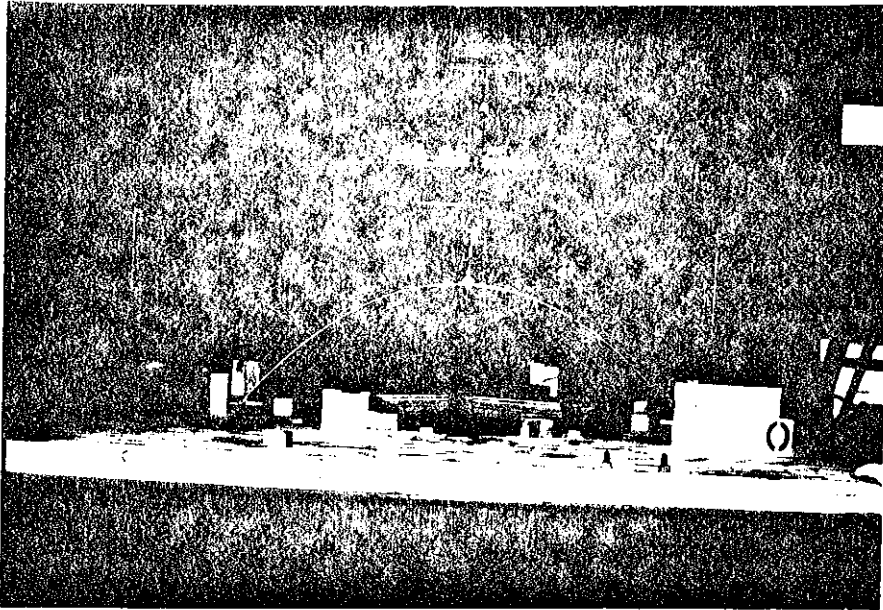
Failure Modes

Figure 8

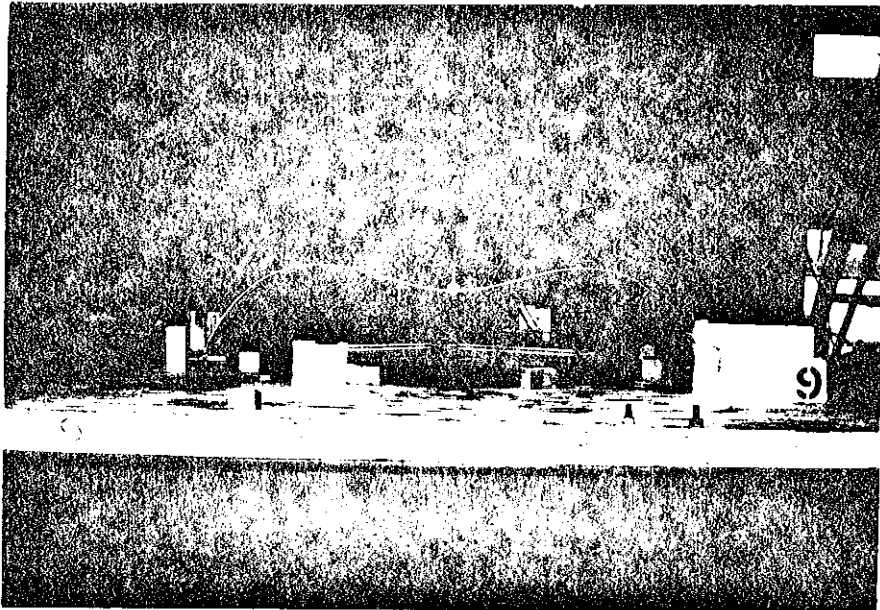


Block and Span Diagram

Figure 9



(a)



(b)

Figure 10

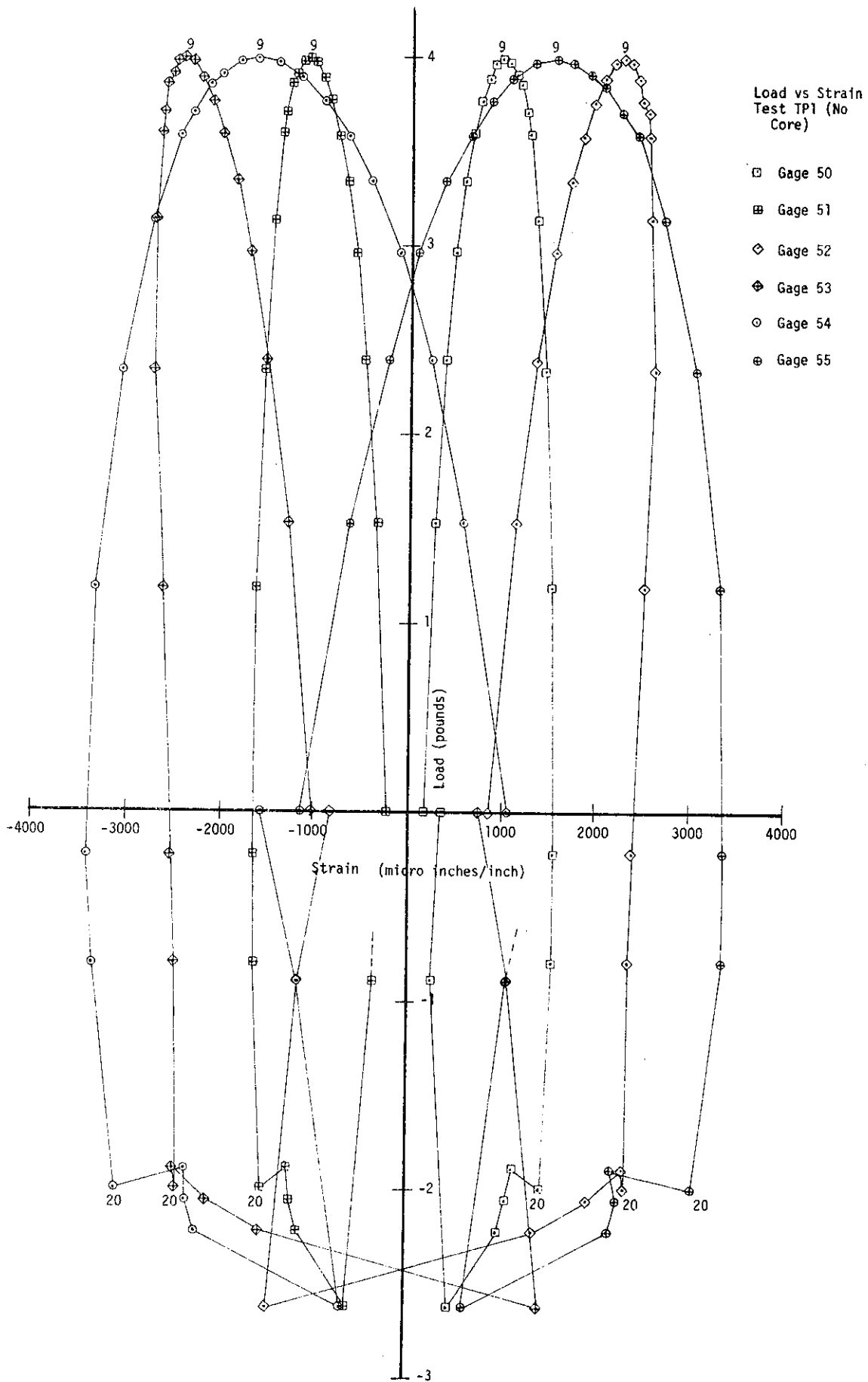


Figure 11

Load vs Center Deflection
Test TP1 (Plain Arch .040" Thick)

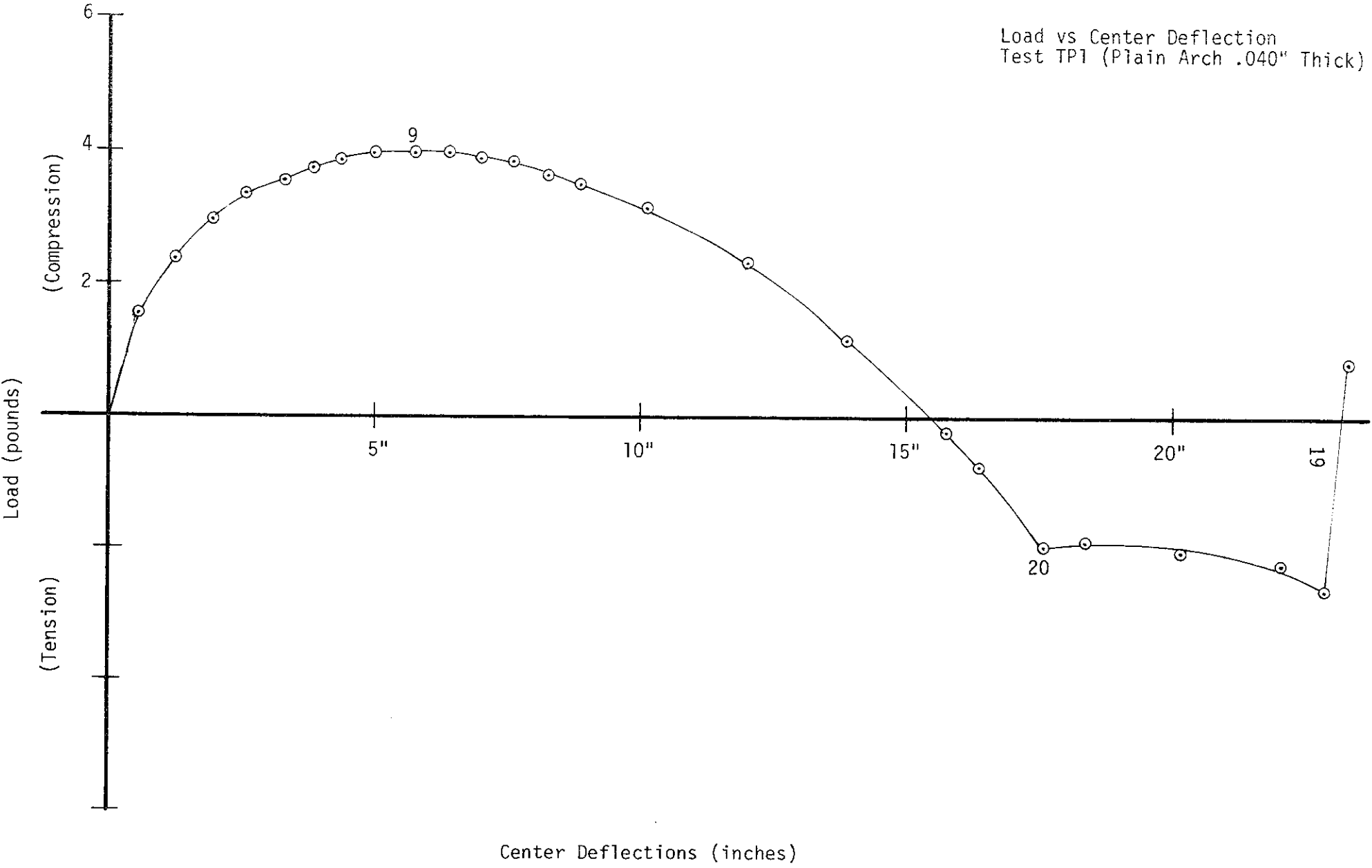


Figure 12

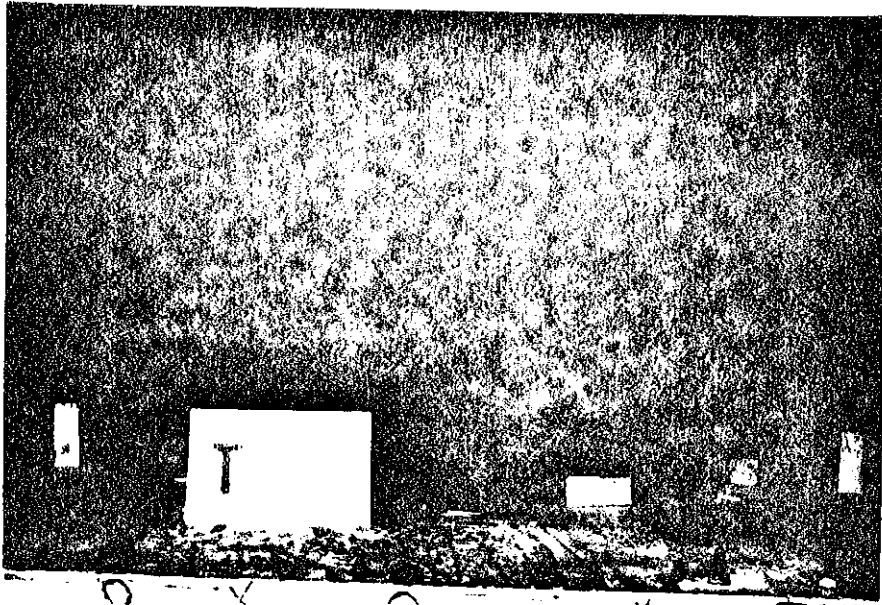
the test was 3.986 pounds.

4.1.2 Model TB I

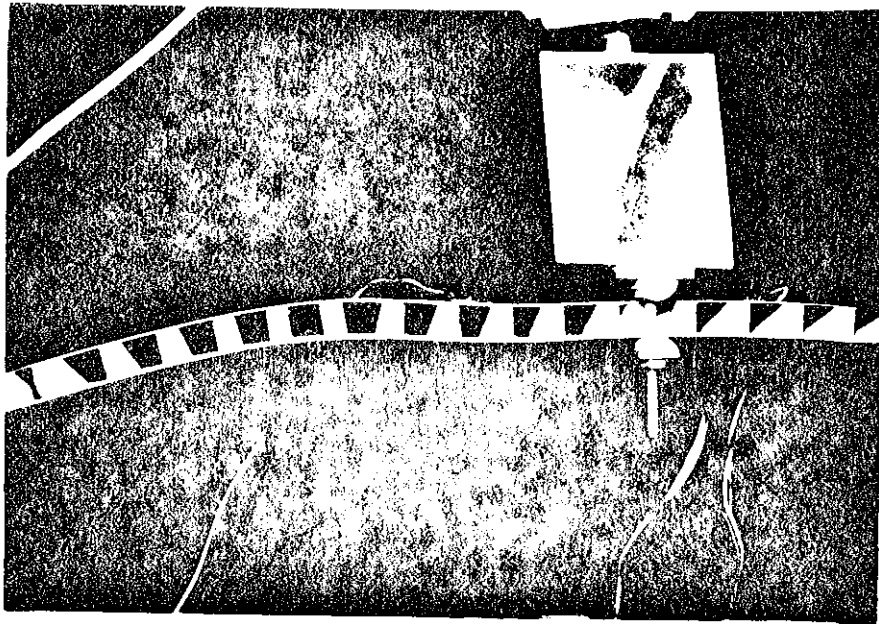
Test TB I was the first sandwich construction tested. The core was made of strips of balsa wood .25 inch wide, .375 inch high, and 3 inches long, which were uniformly spaced along the arch at .625 inch on center. As can be seen in Figure 13a, the erected arch had a curvature which was smooth and symmetrical about the crown.

As the test progressed, no visible changes were noticed in the arch through load point four, but as can be seen from Figure 14, the arch became much stiffer during this period. As load point six was reached, cracking sounds were heard and two pieces of balsa wood were found to be chipped. The load at this stage had just reached 24.66 pounds. Before any more load was applied, failure occurred, resulting in the separation of pieces 1N, 2N, 3N, and 4N from the top skin (Figures 9 and 13b). The mode of failure resembles a shear crimp failure (Figure 8). A shear crimp failure is a specific type of general instability and not a local type of failure, such as intercellular buckling shown in the same figure. In a shear crimp failure the wave length of the buckle is very short due to a low transverse shear modulus in the core.

After failure, the load dropped to 10.13 pounds, a reduction of almost 60%. Strain results are presented in Figures 15, 16, and 17. The local effects resulting from the failure show up dramatically in Figure 17 where gages 42 and 43, located on either side of the crown, are plotted. Gage 42, located on the top facing, above where the failure occurred, jumped from a reading of nearly 500 micro inches/inch to -1000 micro inches/inch. At the same time gage 43, located on the opposite side of the crown exhibited a

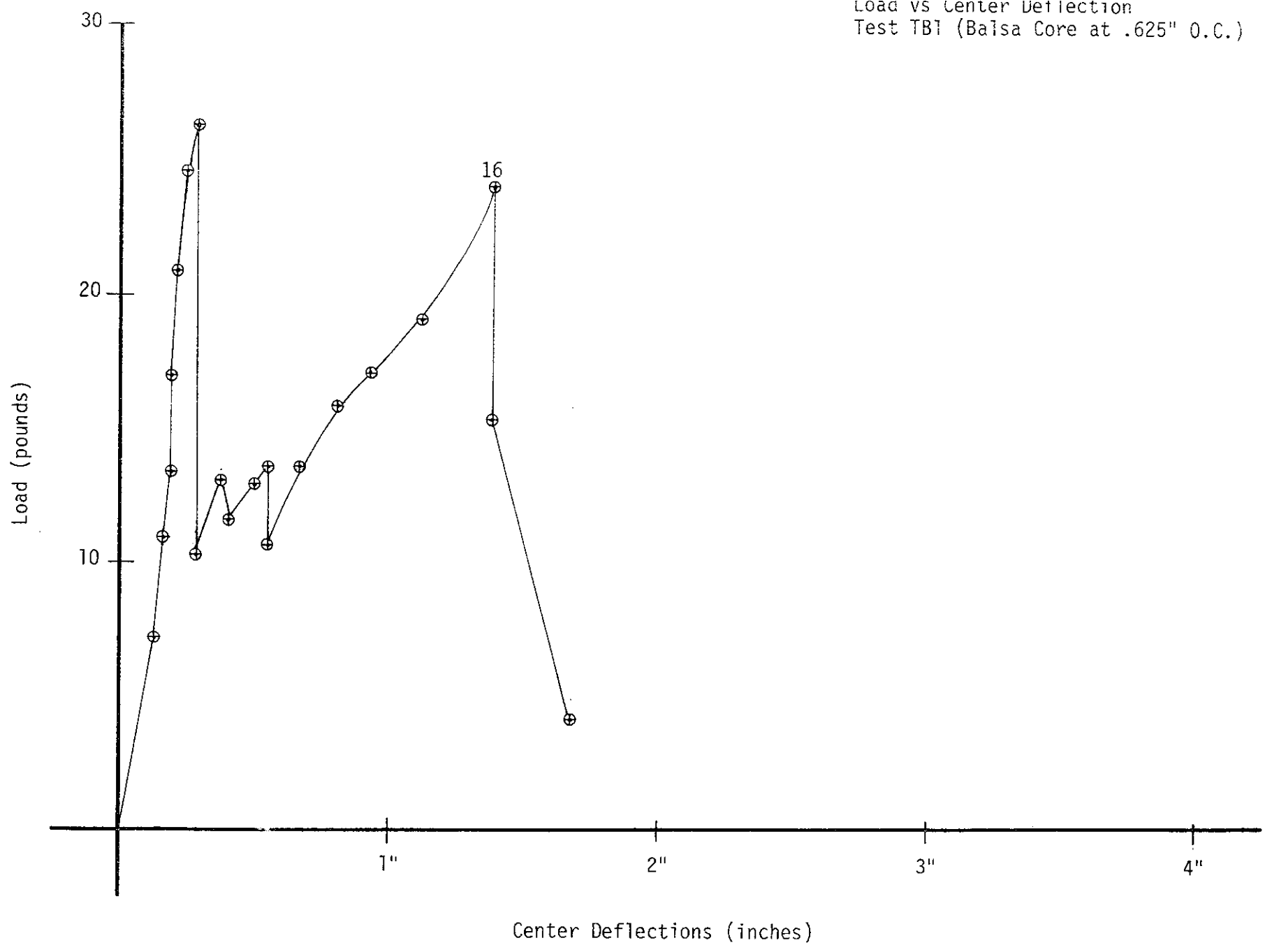


(a)



(b)

Figure 13



Center Deflections (inches)
Figure 14

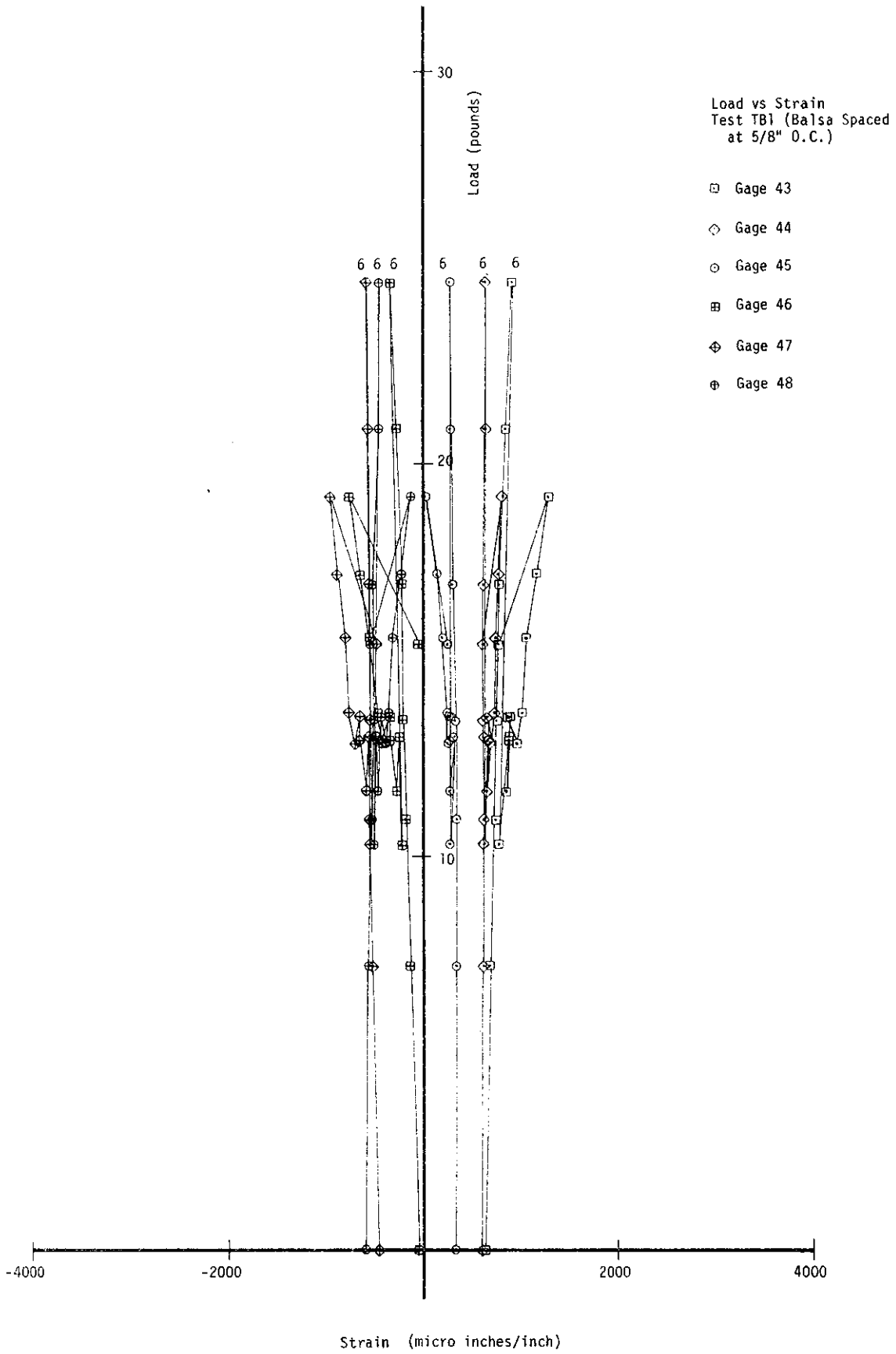


Figure 15

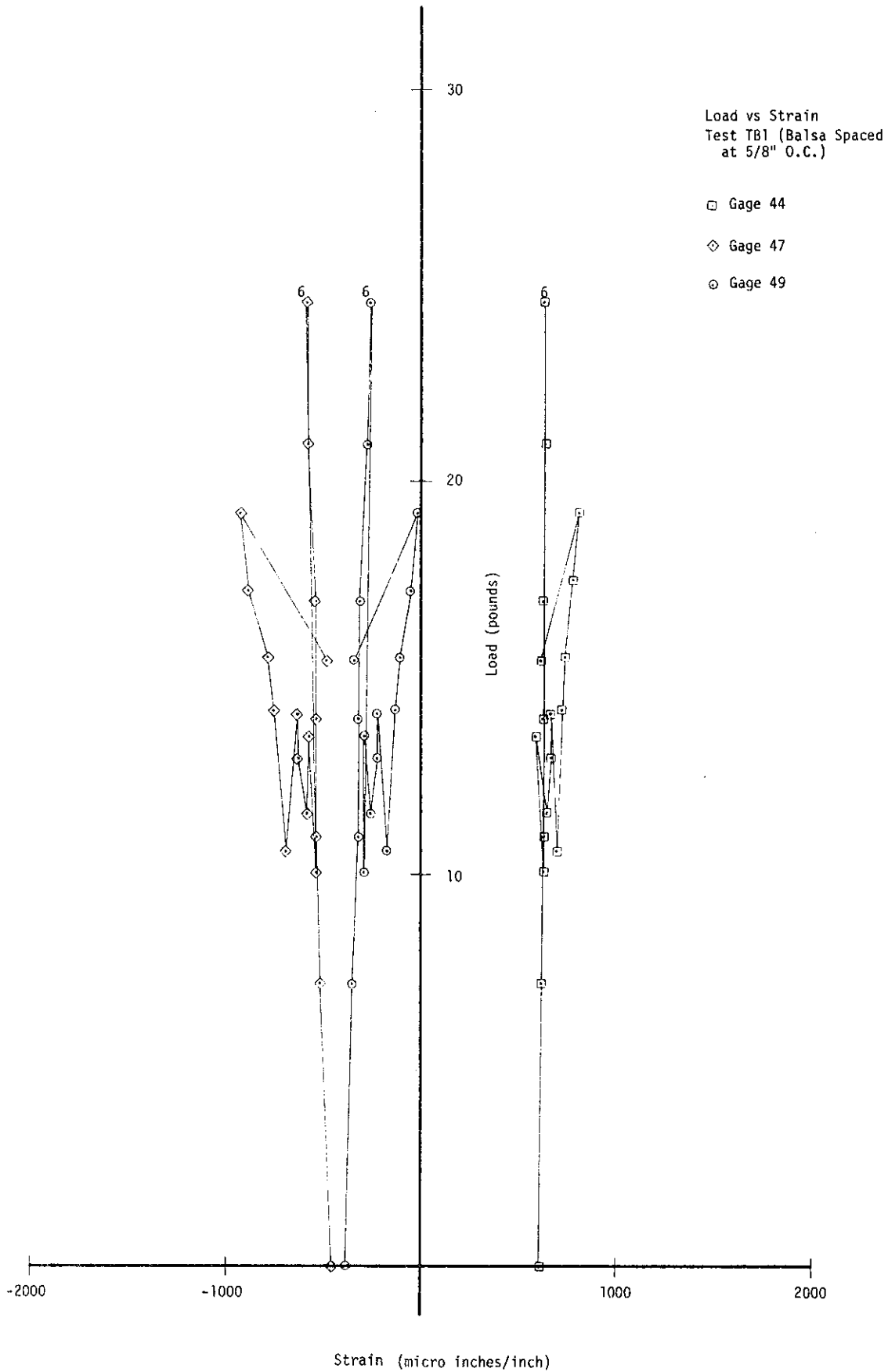


Figure 16

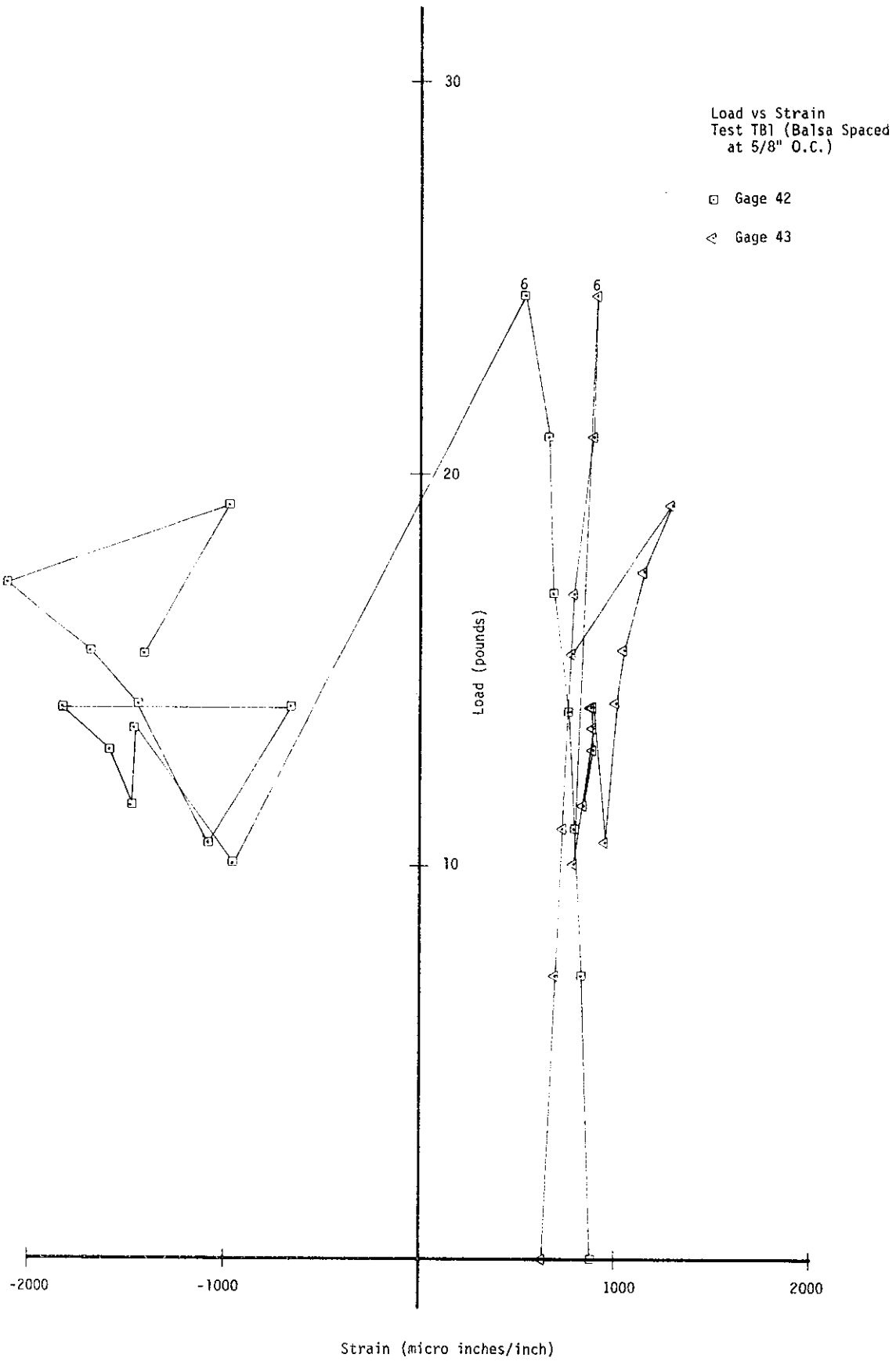


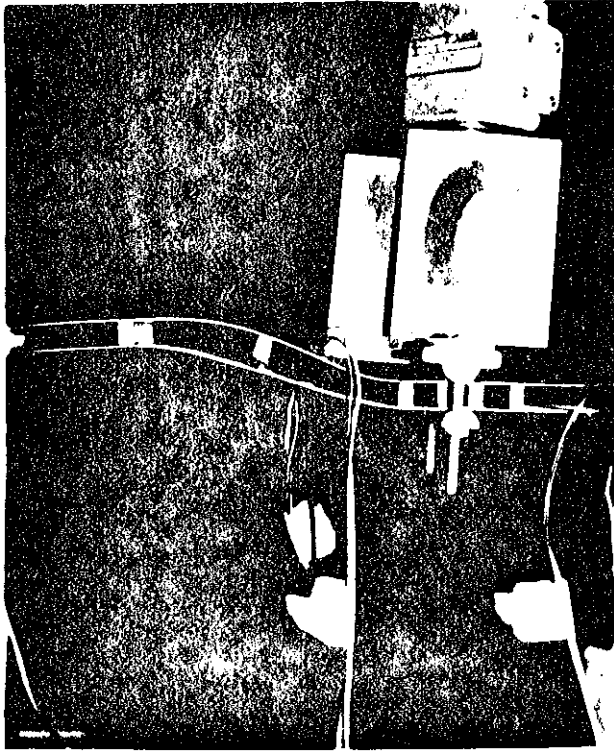
Figure 17

strain just over 200 micro inches/inch.

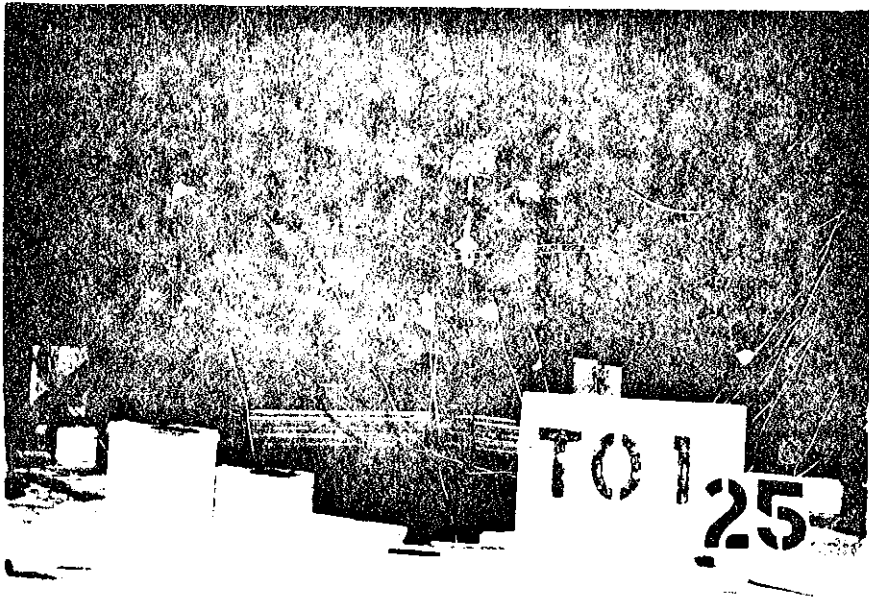
Loading continued with more core separation (5N, 6N) at load points 9 and 11. Figure 14 shows the load building to a peak at these points, but at substantially lower loads than the initial peak. Another significant peak in the load was recorded at load point 16. This peak was achieved as a result of the south leg, which as of yet had no failures in the core. With the failures that had occurred in the north leg, one facing was capable of sliding with respect to the other. This allowed the south leg to rotate about its hinge until checked by the restraint provided at the center. Once this restraint began to take control the load began building again until there was another failure of the bond between the skin and the core on the north leg, combined with a failure of the loading mechanism. After one more load point the test was concluded.

4.1.3 Test T0 I

Test T0 I was conducted on a specimen with an oak core constructed from strips of oak .1875 inches wide by .3125 inches by 3 inches long. The oak strips were spaced at 1.875 inches on center. The curve of the arch initially had some irregularities (Figure 18a) due to the weight of metal clamps that were used in curing this model. As the test began, the load increased linearly with displacement up to load point three as shown in Figure 19. Between load points three and nine the increase in load per unit displacement became less. By load point nine, at which point the load was 22.9 pounds, there was noticeable wave-like deformations in the three spans on either side of the crown due to the restraint provided by the core (Figure 18b). These deformations are reflected in the strain gage readings on either side of the crown. Figures 20 and 21 show that gages 44 and 47, located on



(c)



(d)

Figure 18

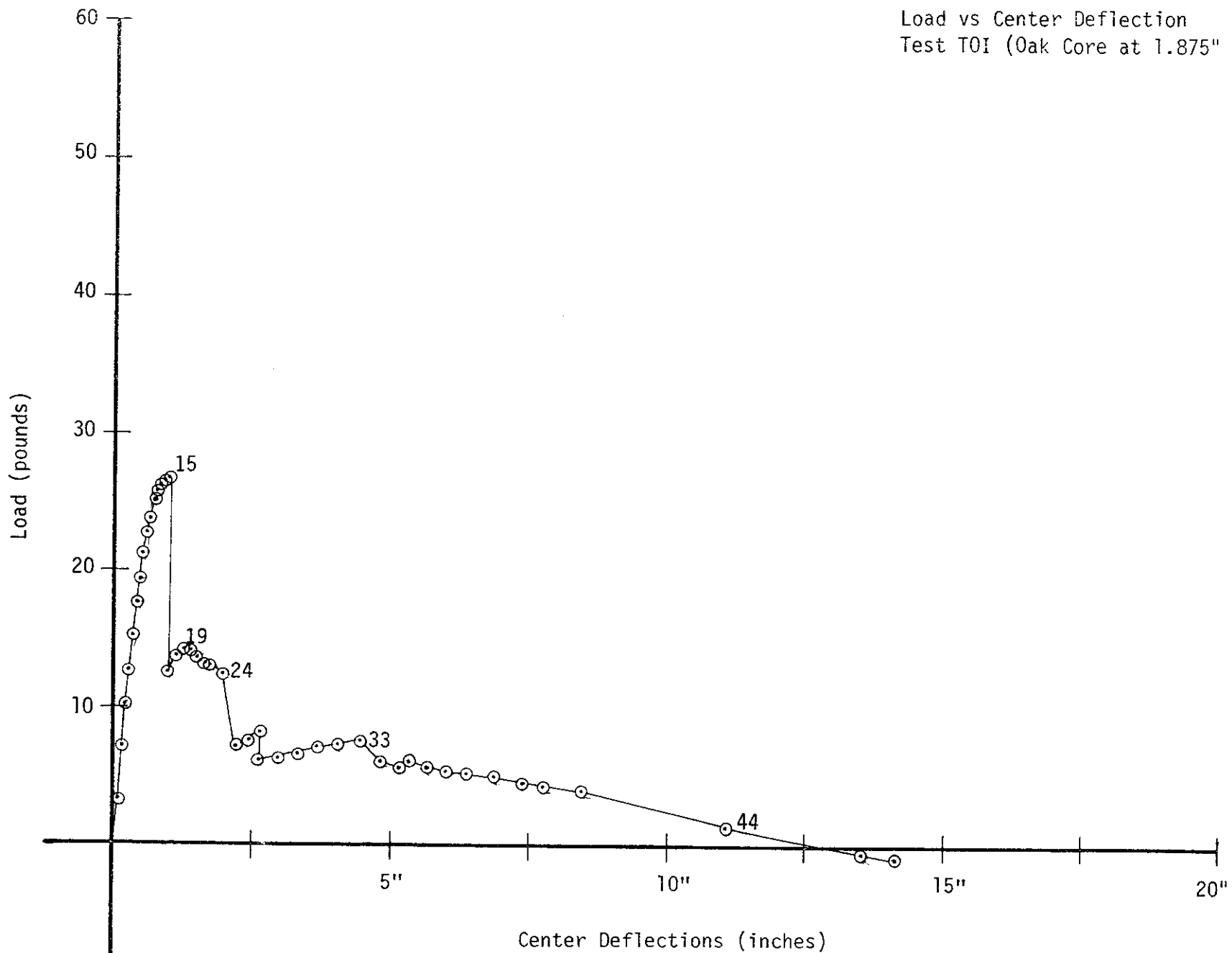


Figure 19

Load vs Strain
Test T01 (Oak Spaced
@ 1 7/8" O.C.)

- Gage 47
- ⊞ Gage 44
- ◁ Gage 42
- ▷ Gage 49
- Gage 51

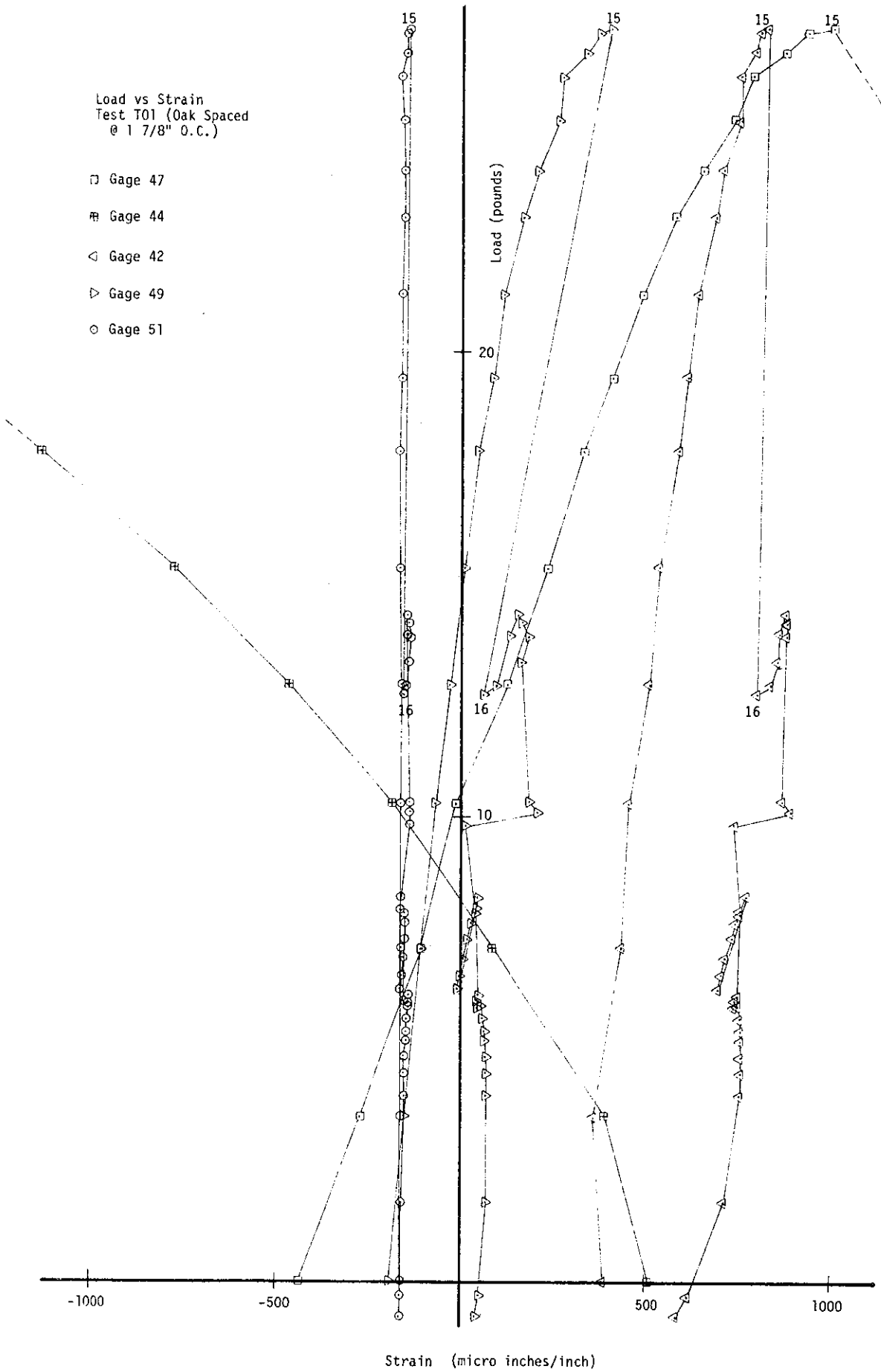
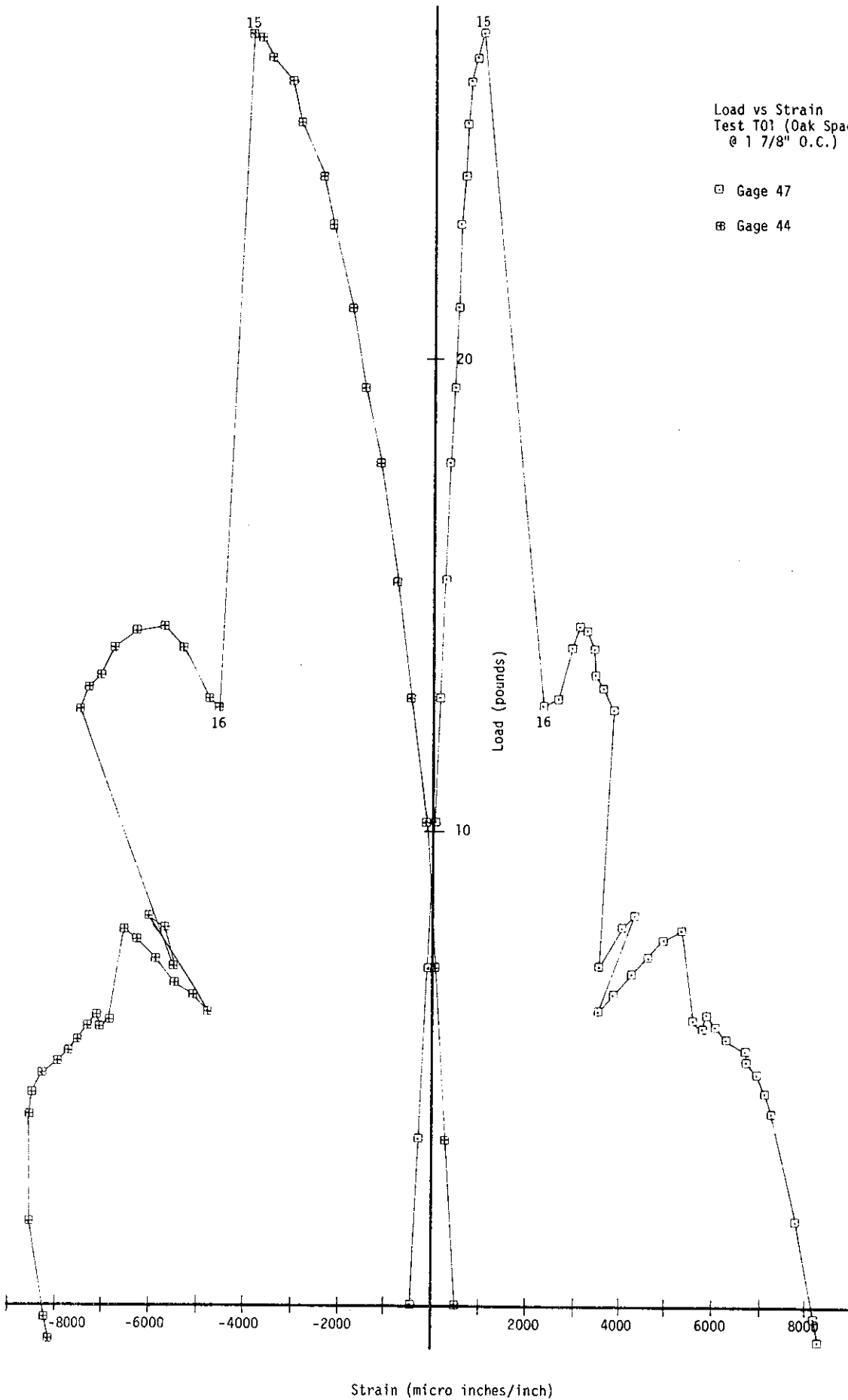


Figure 20

Load vs Strain
 Test T01 (Oak Spaced
 @ 1 7/8" O.C.)

□ Gage 47

⊞ Gage 44



Strain (micro inches/inch)

Figure 21

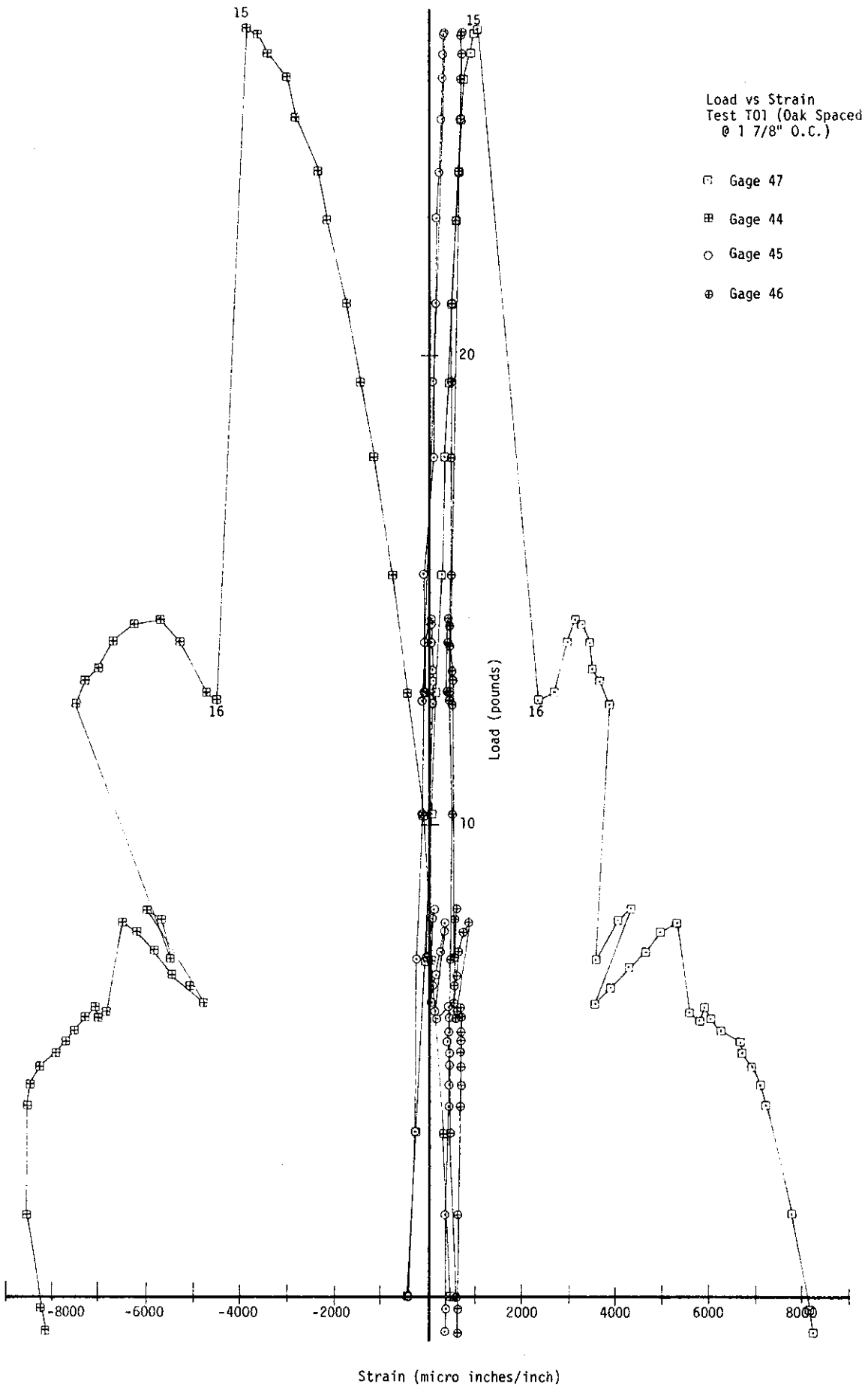


Figure 22

the top and bottom faces next to the crown, increased in strain more rapidly than did those gages which were located elsewhere on the leg. The deformation at this stage resembles the intercellular buckling shown in Figure 8. Intercellular buckling is a localized failure mode which can occur only when the core of the panel is not continuous. With this type of behavior the cell walls act as supports and the facings buckle between them. Figure 18b shows that there is a complete wave between elements of the core, occurring most predominantly in the top face. Intercellular buckling often precipitates face wrinkling, in which the facings buckle in short wavelengths which are not confined to individual cells of the core. This type of instability develops a strain in the core material normal to the facings and could result in a failure which is either a compressive or tensile failure of the core itself or the bond between the core and the facing.

Between load points 15 and 16, while the load was 26.95 pounds, there was a combined shear and tension failure of core piece 1S. As a result of this combined action the oak piece separated from the bottom face and moved approximately $\frac{3}{16}$ inches south and $\frac{1}{8}$ inches up relative to the bottom face. This failure released instabilities which had developed elsewhere in the arch. At the location of the failure, the arch no longer acted as a composite member, but instead the faces acted as independent member, where each face took a portion of the load.

Upon failure, gage 49 located half way up the bottom surface of the south leg, registered a drop in strain of nearly $\frac{1}{3}$ of what it had measured, while the top gage showed an insignificant drop in strain, by comparison. At the same time, the gage at the same location, but on the opposite leg, gage 43, also registered an insignificant drop in strain. After the next load point, one could tell that the bottom face of span 7N was buckling as a

release mechanism for that leg.

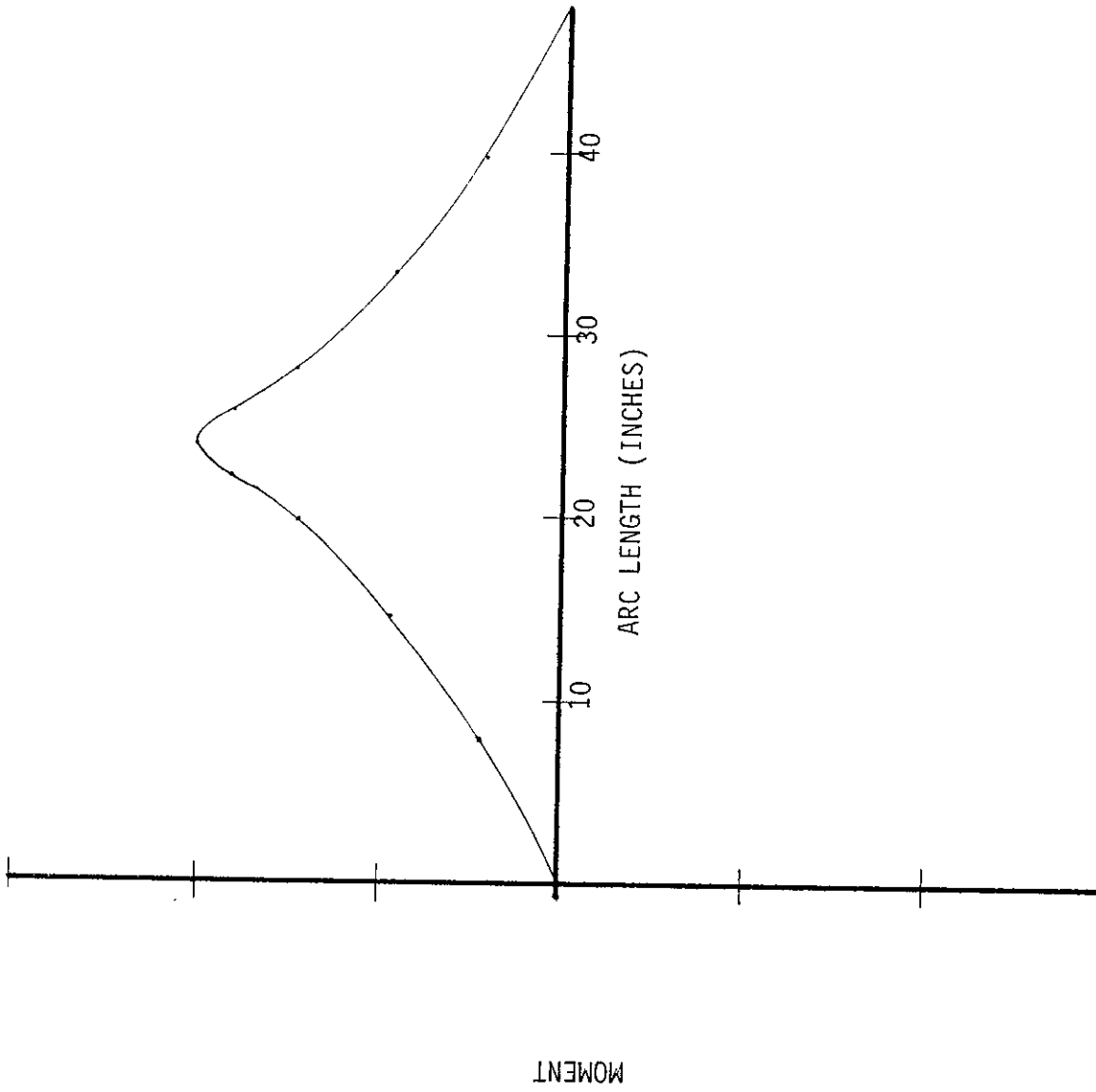
After the initial failure, the load rose again until load point 19, Figure 19, when the load was 14.37 pounds, where it began to slowly drop off as span 7N continued to buckle. At load point 24, oak piece 2S failed accompanied by another drop in the load. Load began to pick up again and reached a peak at load point 27 where another piece, 3S, failed resulting in another drop in load. Each successive peak attained was substantially lower than the next as the test progressed. Following load point 28, the load increased to load point 34, where the arch shifted slightly to the north. From this point on the load dropped with each successive load point. By load point 44, the crown of the arch had been displaced to the point where it was now even with the top of the platform. A compressive load of 1.68 pounds was recorded at this stage. The arch was taken through two more load points, after which time a tensile load of .7 pounds was registered by the load cell. At this point the load cell was detached from the arch and raised back to its original position. The arch rebounded to a position similar to that which it had started, but with some permanent deformation (Figure 18d).

4.1.4 Test T0 II

The spacing used in test T0 II was based on two results. One, the results of tests TB I and T0 I, in which it was shown that the close spacing used in Tb I caused a core failure, while the wider spacing used in T0 I caused local wave-like deformations to develop near the crown, resulting in a core failure. The results of an analytical investigation of the arch, assuming small deflection theory, was the second result. For this investigation a uniformly distributed live load was applied to the arch. While this is not the type of loading which would be applied during the testing, it more closely approximates loading

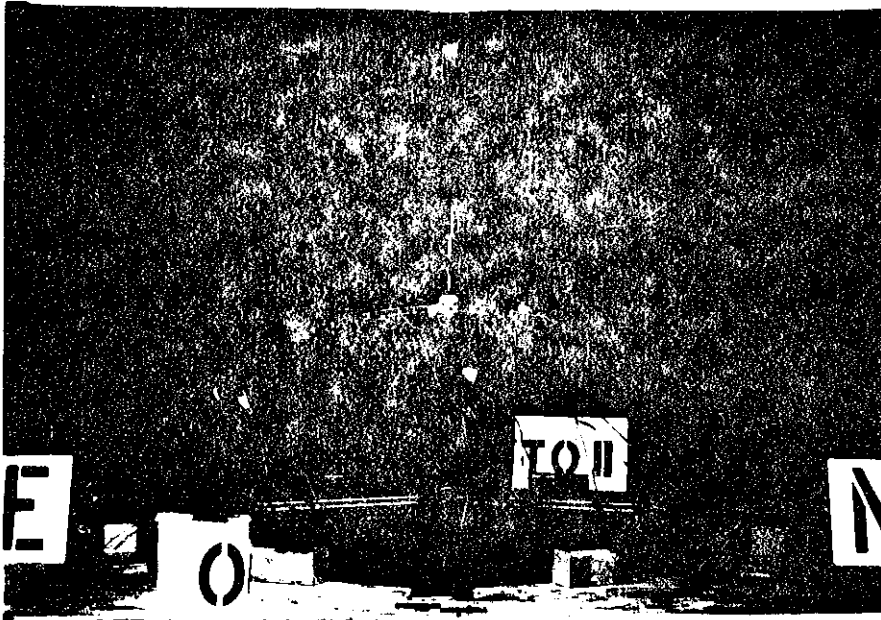
conditions which might be experienced in the field. A plot of moment versus arc length is shown in Figure 23. From this plot it can be seen that a closer spacing near the crown would be advantageous. This would place more core material in the region which requires more shear resistance. Based on these two results, it was decided to use a spacing which increased linearly outward from the crown. The spacing was .625 inches center to center in the first span, while the widest span was 1.75 inches, with each intermediate span increasing by 1/16 inch. By using this spacing it was hoped that the local deformations experienced in T0 I would be eliminated.

As the test began, it was noted that the use of wooden clamps eliminated the irregularities which were present in T0 I (Figure 24a). At load point three there were some cracking sounds, but no visible signs of bond or core failures. It is readily apparent from the load versus displacement curve (Figure 25) that this sandwich arch is much stiffer than those previously tested. Figures 26 through 29 show load versus strain curves for T0 II. Figure 27 shows that following load point three, there was a marked change in the behavior of gages 45 and 48. At load point four, a slight dip was noticed at the crown and there was a drop in the rate at which the load was increasing. Load point five brought with it signs of a possible failure developing in span 3S (Figure 24b). There was still no sign of any core or bond failure. Load point six was reached and readings were taken with only span 3S showing wave-like deformation. Figure 27 shows that gages 45 and 48 had gone from tension to compression and compression to tension respectively. Before any more load could be applied, a bond failure developed at 3S and the test was discontinued. It appears that the spacing used had performed as desired in eliminating most of the wave-like deformations which developed near the crown in test T0 I.

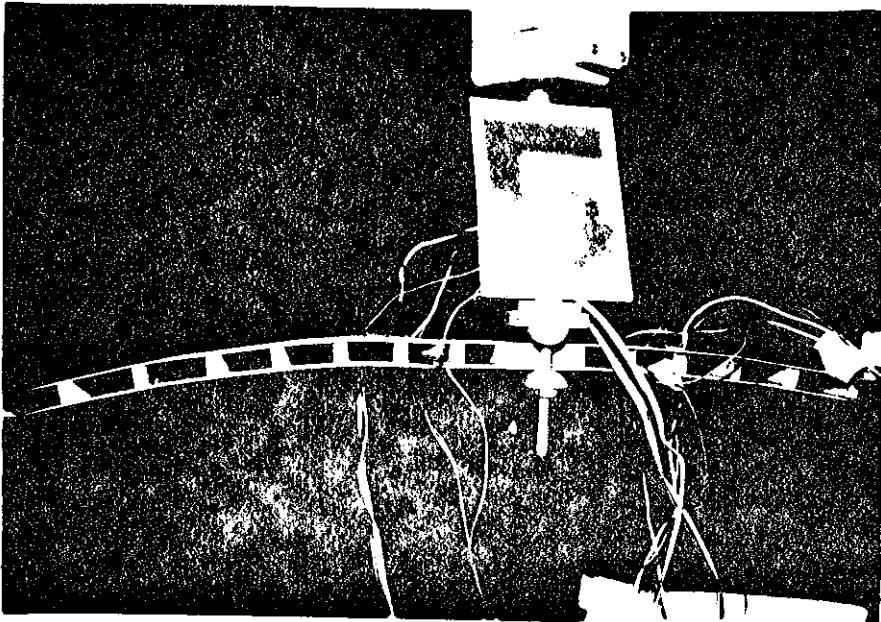


Moment Versus Arc Length For
Uniformly Distributed Live Load

Figure 23

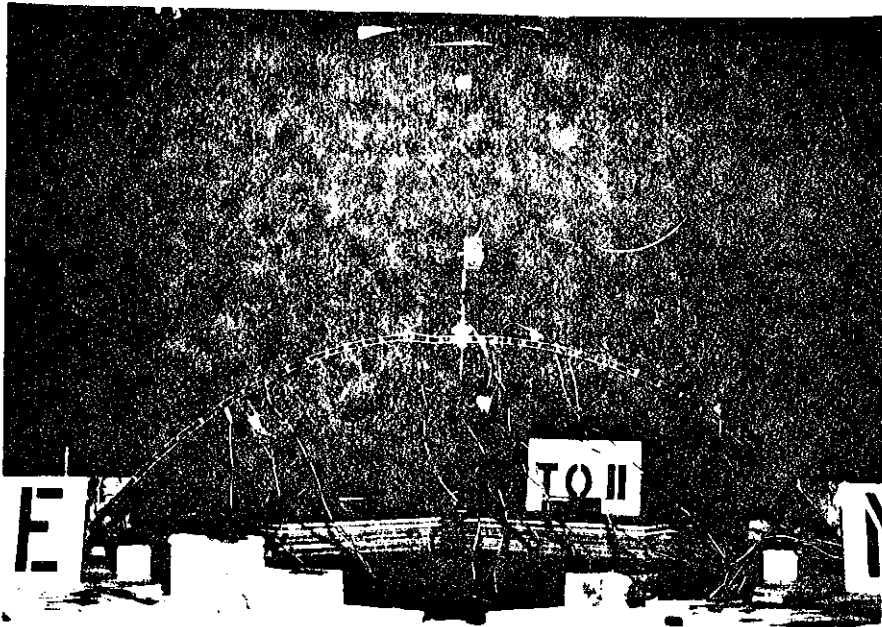


(a)



(b)

Figure 24

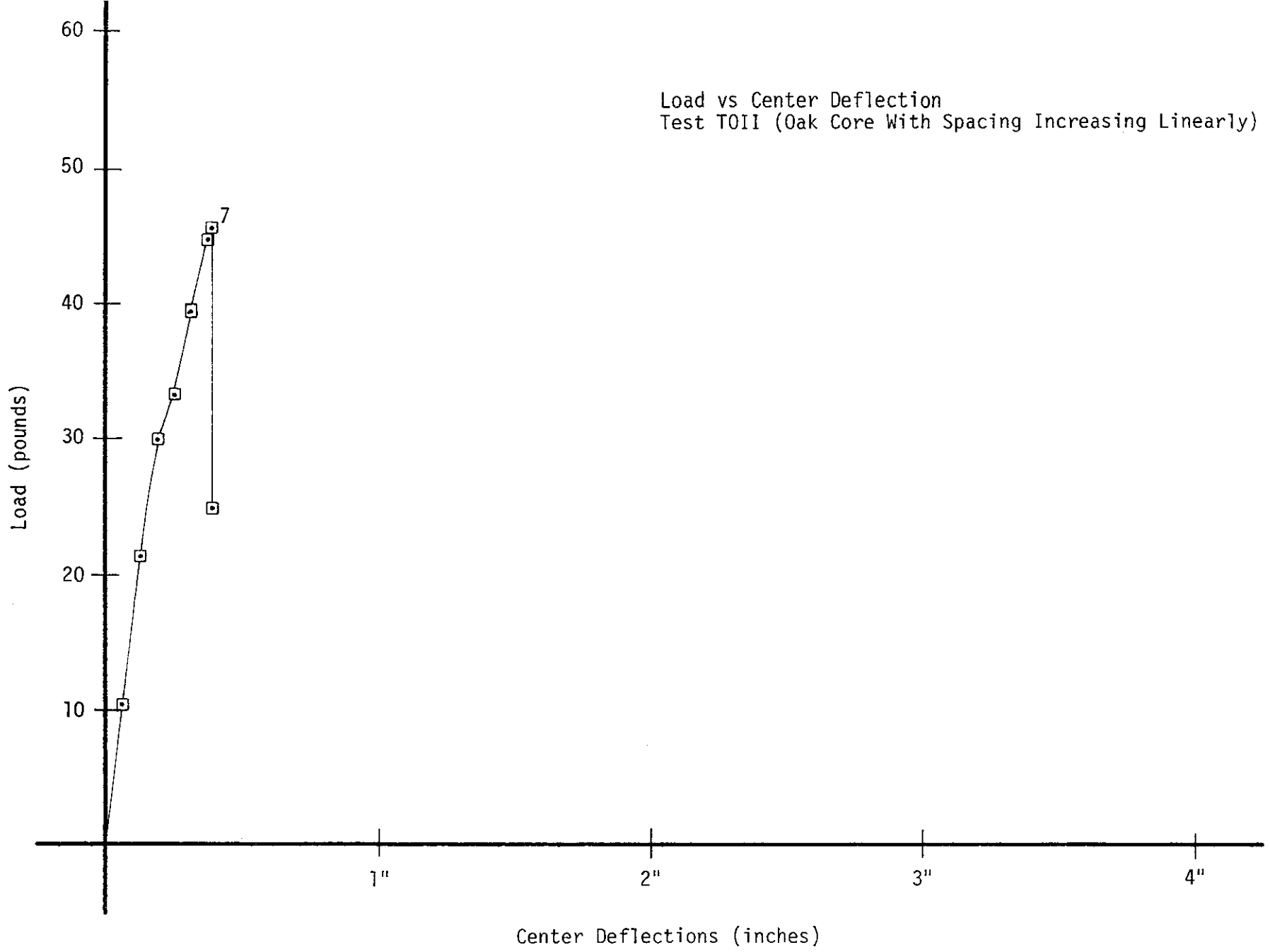


(c)



(d)

Figure 24



Center Deflections (inches)

Figure 25

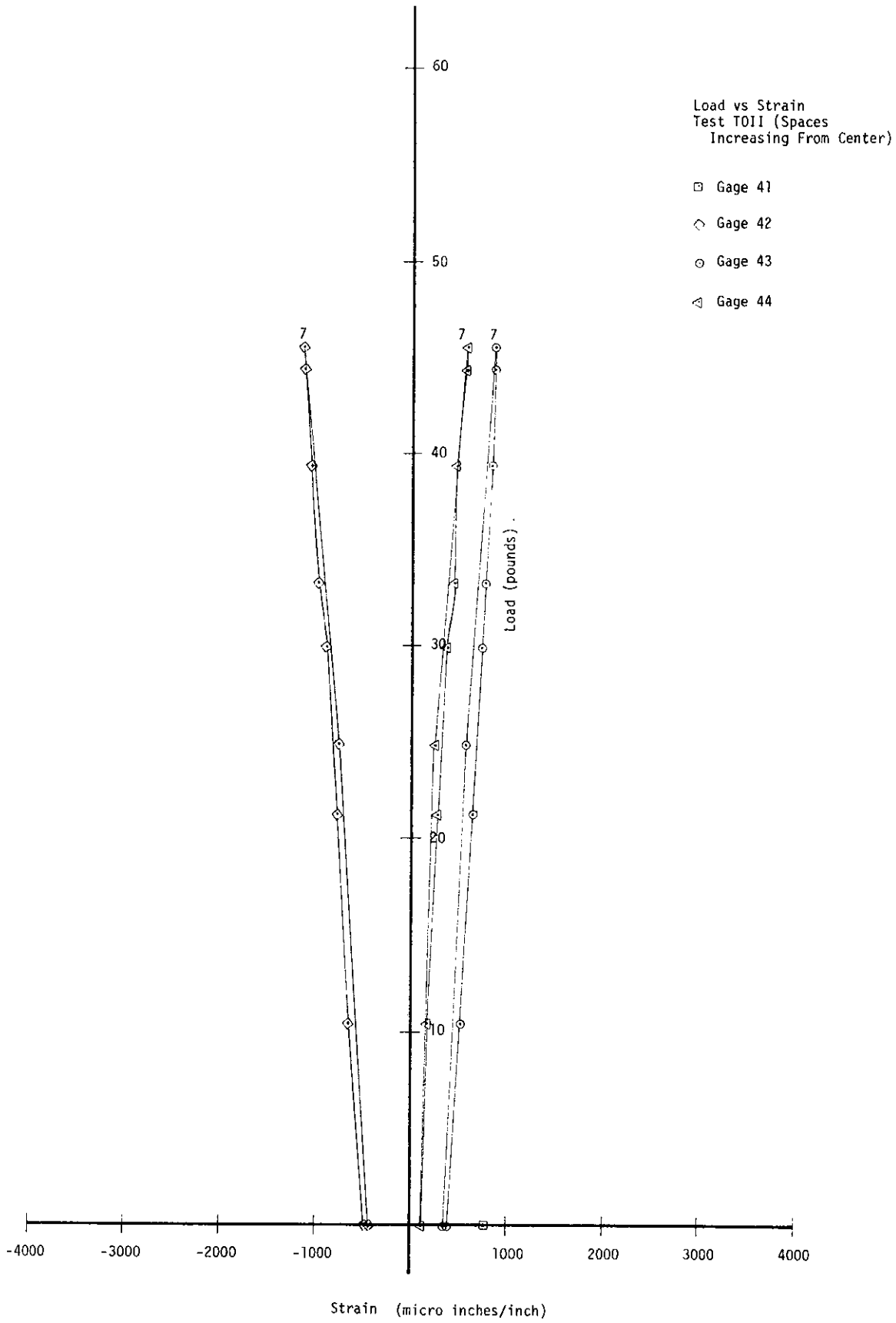


Figure 26

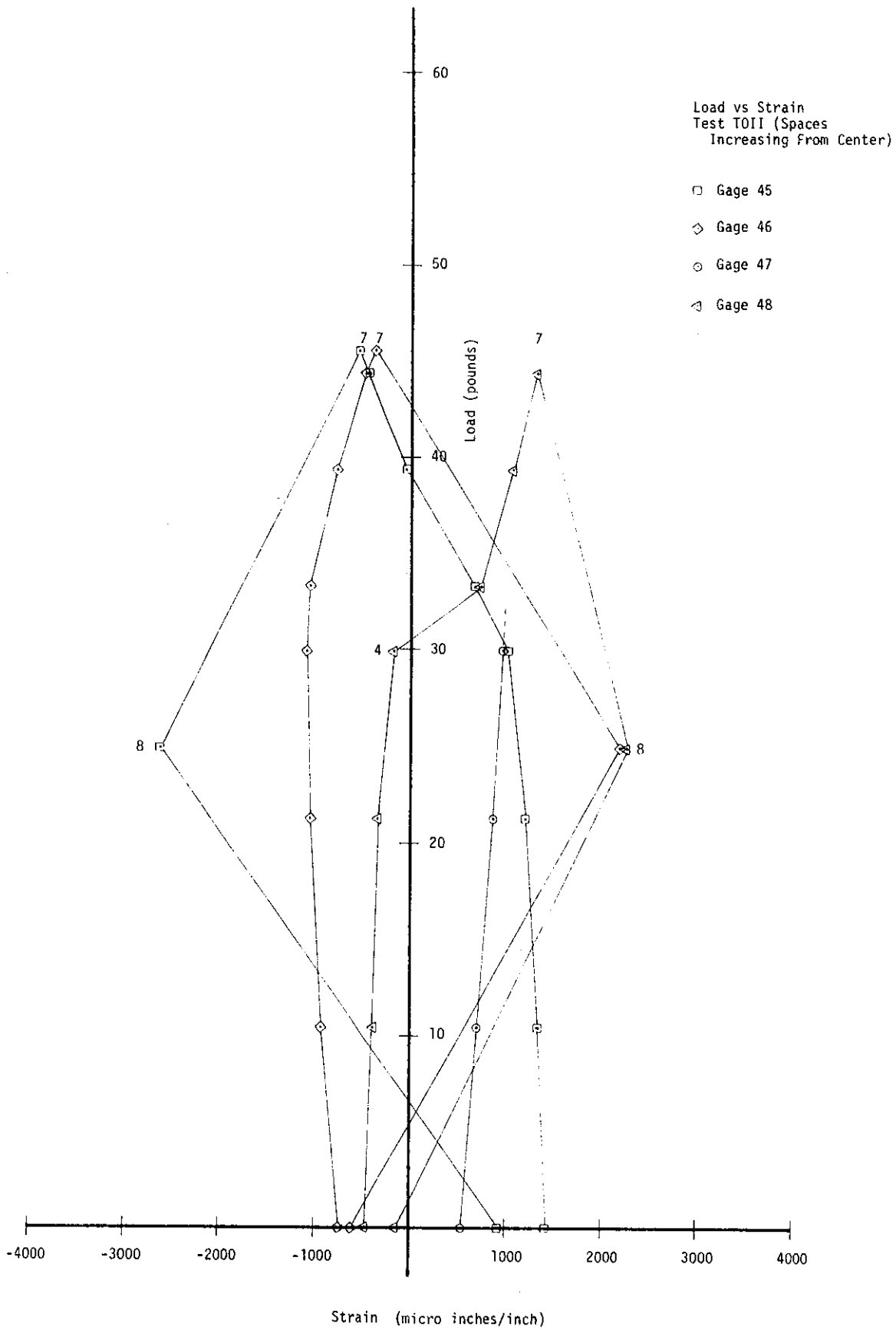


Figure 27

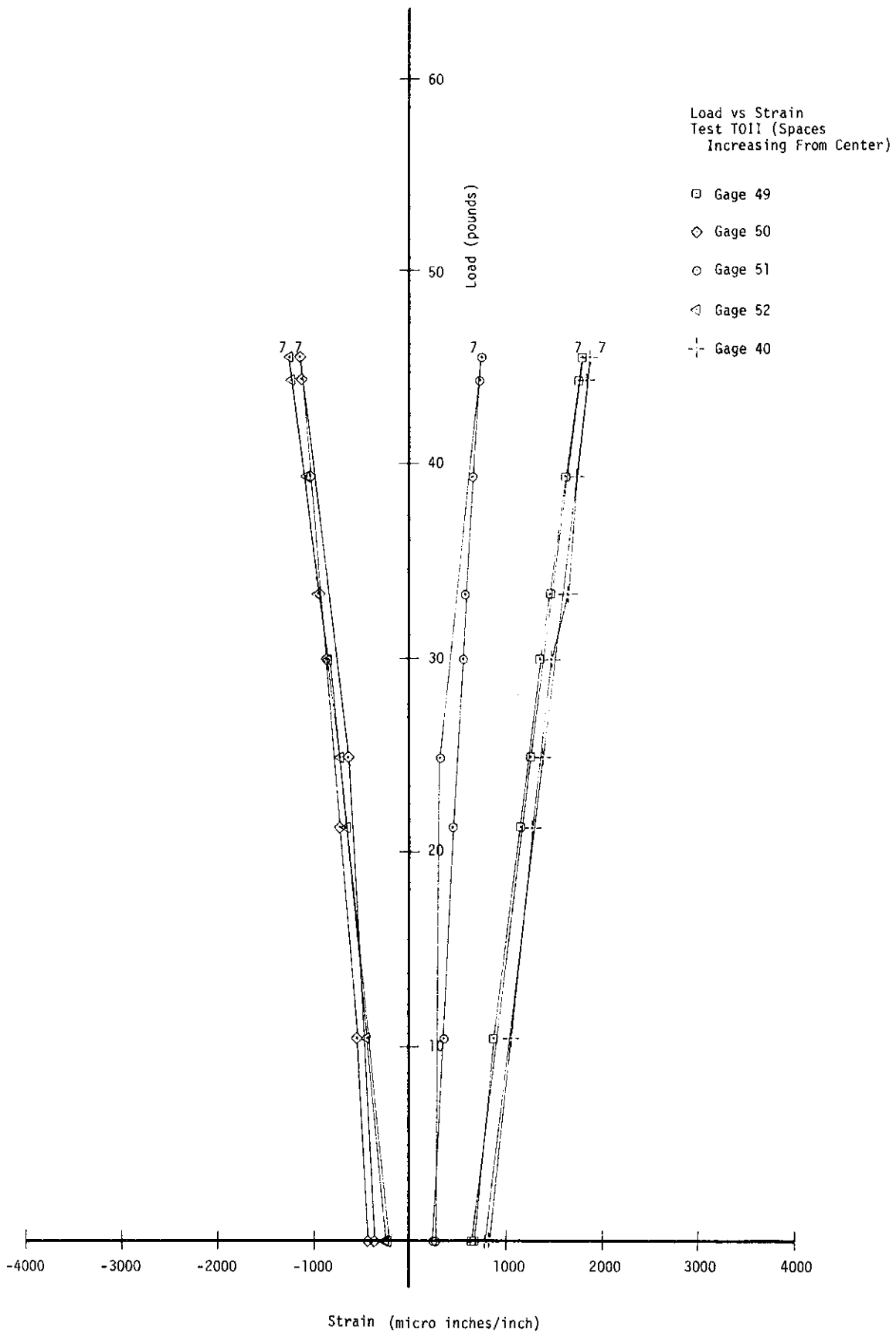
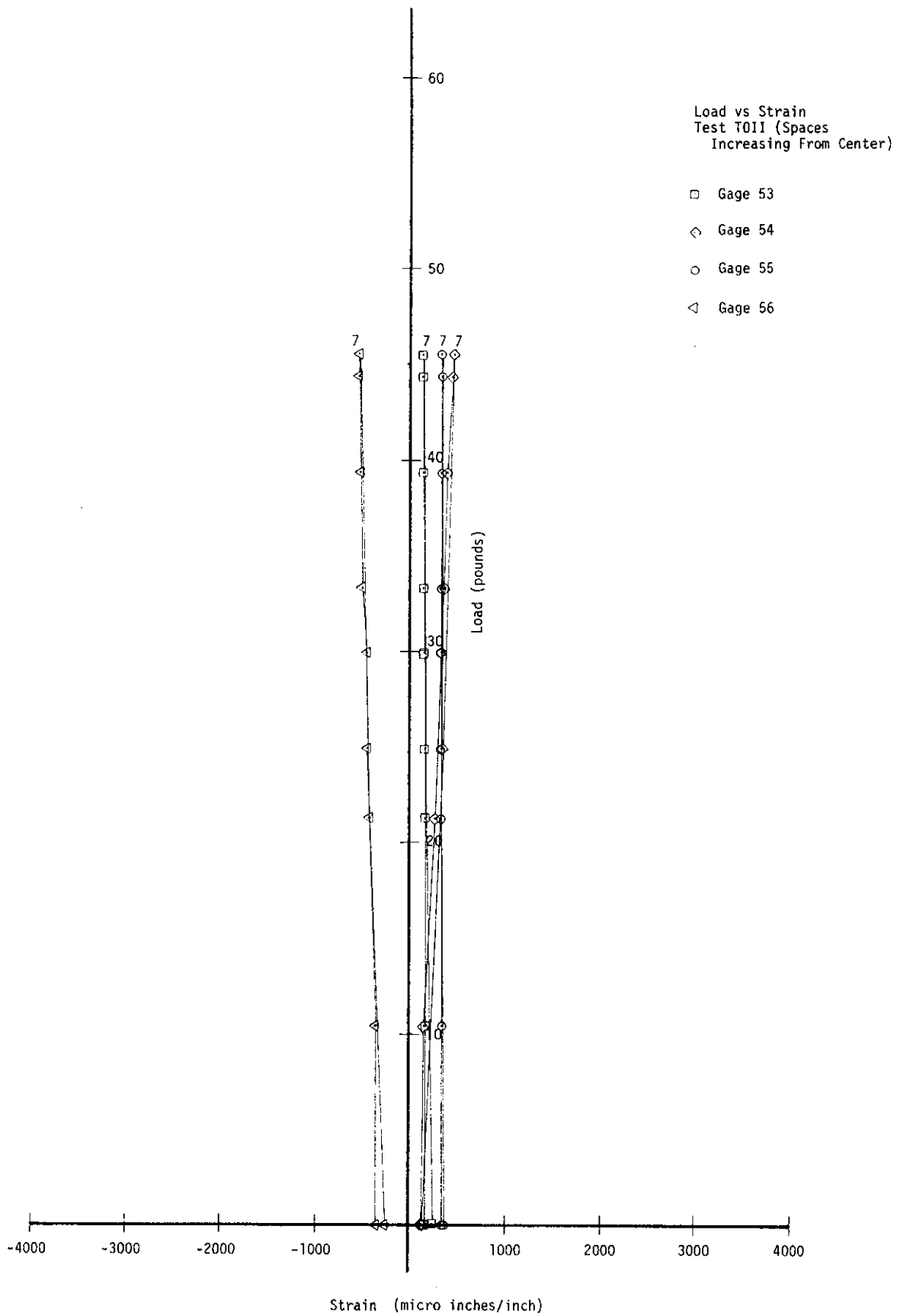


Figure 28



Strain (micro inches/inch)
Figure 29

4.1.5 Test T0 III

After obtaining the results from test T0 II and examining them, it was evident that a larger load, as well as a different mode of failure, could be achieved if a better connection could be developed between the core and the facings. The same spacing used in T0 II was used in T0 III. In an attempt to develop this bond, the core was glued and bolted to the facings as shown in Figure 30a. The initial curve was smooth, with no signs of any irregularities.

The test began with the load behaving linearly up to load point four, at which time the load was 35 pounds. After this point, the increase in load tended to decrease per unit deflection (Figure 31). By load points seven and eight, some flattening of the crown was observed and cores 2N and 2S separated from the facings at the edges. This caused a drop in the load on the arch and a redistribution of the strains, as can be seen in Figures 32-35. Upon reaching load point nine, the load was 60.64 pounds and wave-like deformations were noted across the total length of the arch. These deformations (Figure 30b) were more pronounced near the supports. This behavior continued through load point ten, after which the bottom facing in span 17N experienced a local buckling failure, resulting in permanent deformations (Figure 30c). The deformations over the remainder of the arch were relieved after the buckling of span 17N. The buckling destroyed the symmetry of the arch, allowing the north leg to move out. Upon release, the arch returned to a position similar to its original shape but with permanent deformation in span 17N (Figure 30d).

It is readily apparent from this test that using the bolts combined with the glue provided a much stronger bond and core. This forced the failure into the facings and resulted in the buckling of span 17N.

Upon performing an analytical investigation of a plain arch, using small

deflection theory, it can be seen that near the supports of the arch, the resulting moment puts the bottom face of the arch in compression. This combined with the axial load acting on the arch and the increased spacing of the core near the supports resulted in the buckling of span 17N. Figure 36 shows a plot of moment versus arc length for a single concentrated load at the center of the arch.

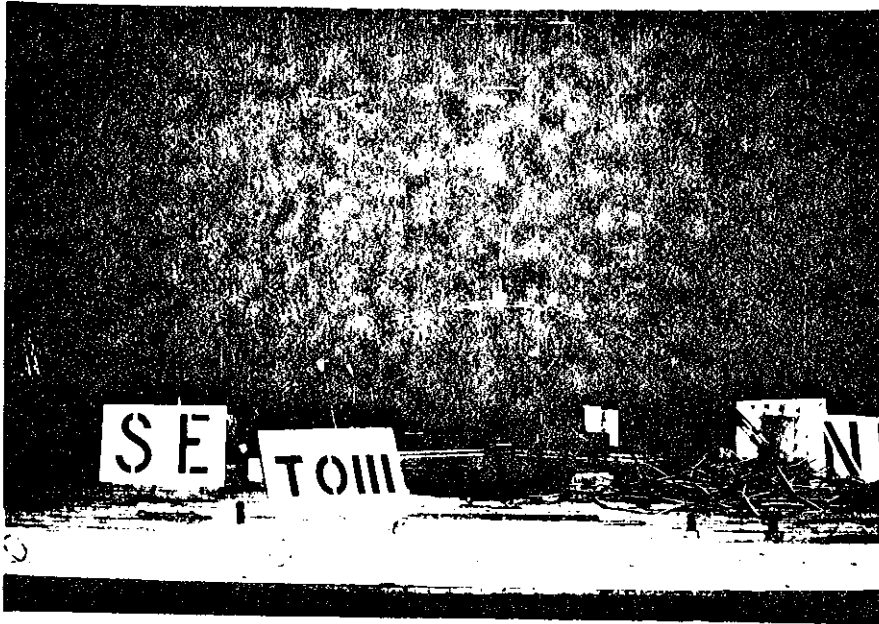
5.2 Shear Test Results

Shear tests (Figure 37) were performed on both the balsa wood core and the oak core according to ASTM standards (4) with the following exception; only two specimens of each type were tested as opposed to the five recommended by the standards. The specimens were constructed using .1875 inch thick aluminum for the facing. For the balsa wood test, the core was made from strips of balsa wood which were .25 inches wide, .375 inches high, and 2 inches long and were spaced at .625 inches on center. The oak core was made from strips of oak which were .1875 inches wide, .3125 inches high, and 2 inches long. These strips were also spaced at .625 inches on center. The same type of adhesives and curing process used in the construction of the arches was used for the shear tests. Both types of specimens were 2 inches wide by 5.3125 inches long, with nine blocks of wood in each.

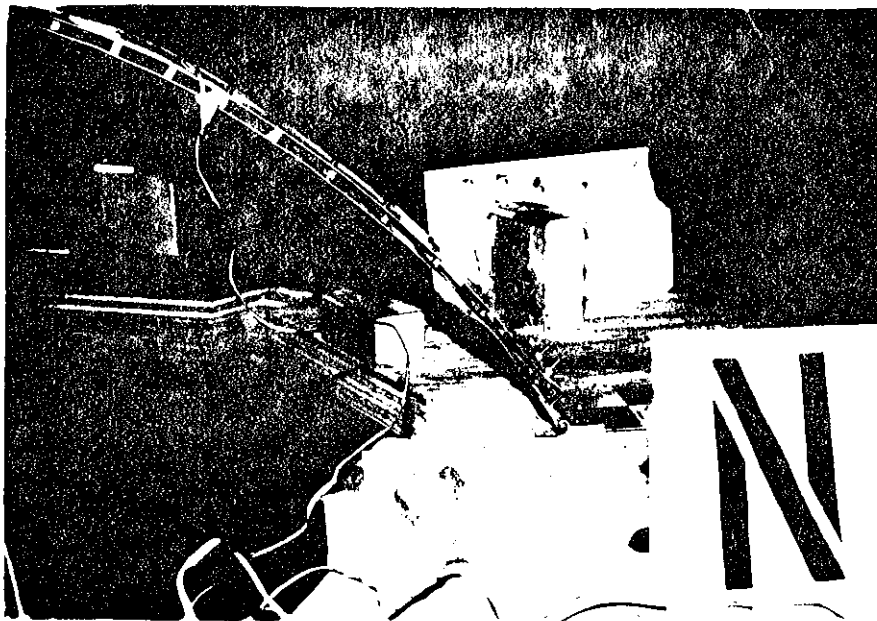
The results of the tests are presented in a load versus deflection plot shown in Figure 38. The balsa wood core failed due to shearing of the core followed by bond failures, while the oak failures were predominantly bond type failures with a small number of wood blocks being sheared.

The shear modulus of the core was computed using ASTM formula (4);

$$G_c = \tau/\lambda$$

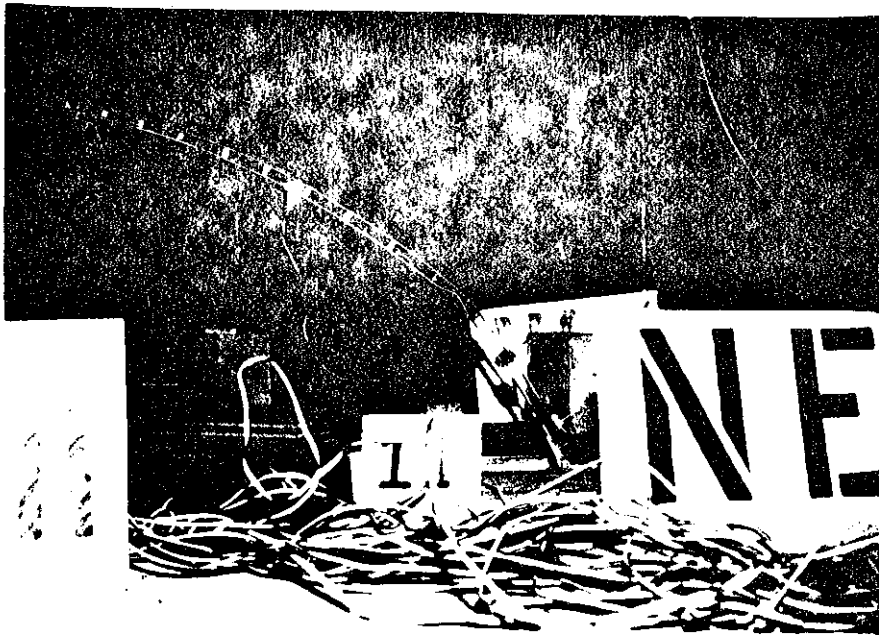


(a)

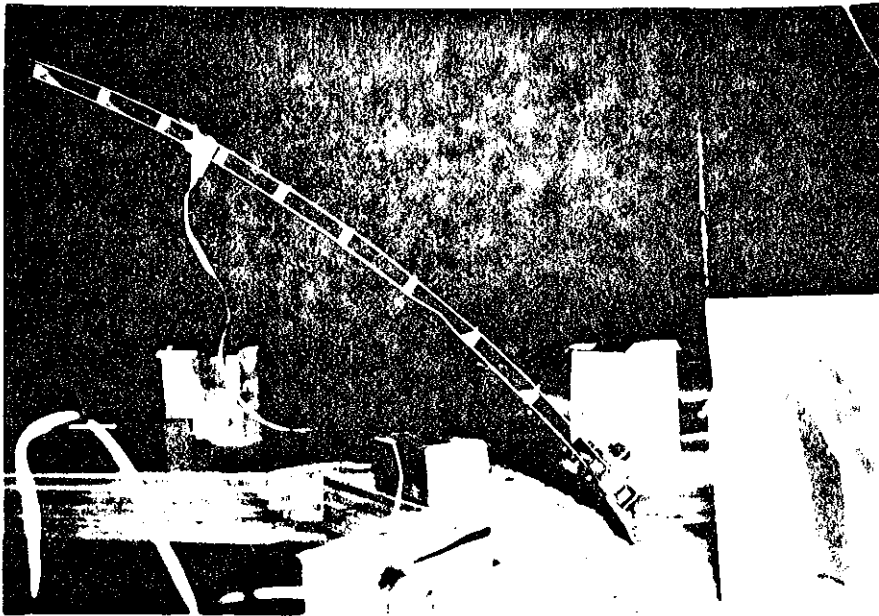


(b)

Figure 30



(c)



(d)

Figure 30

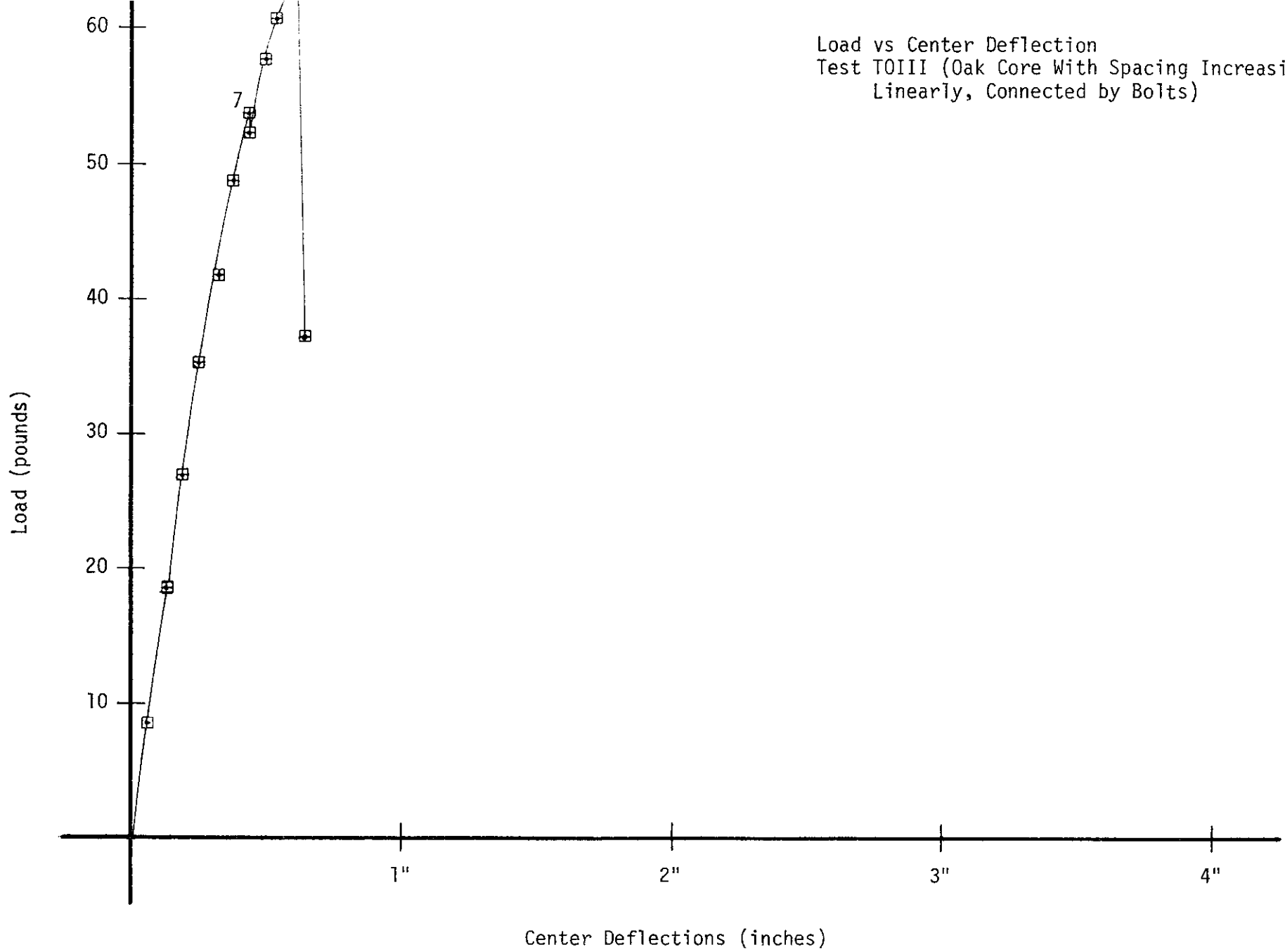


Figure 31

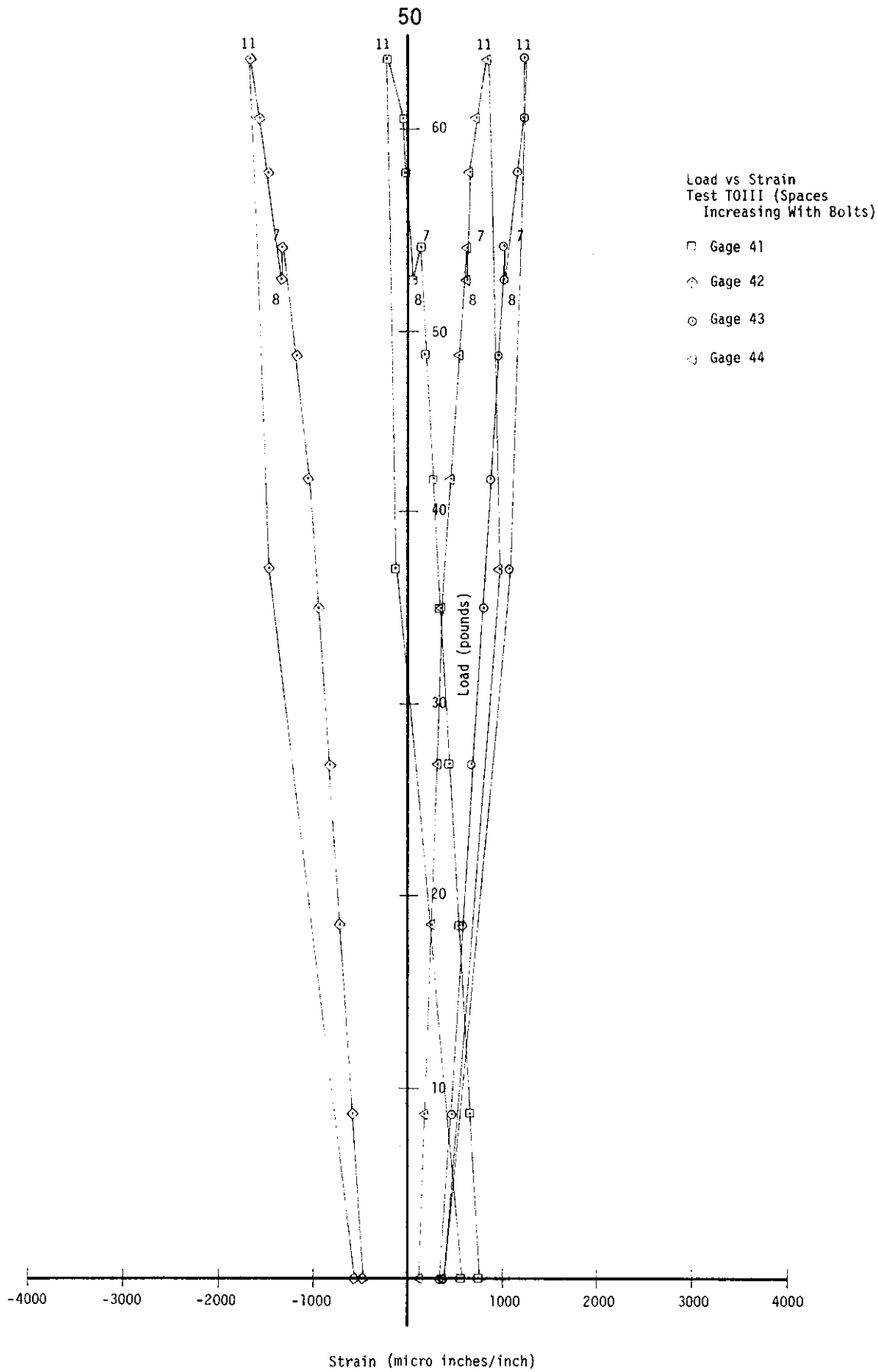


Figure 32

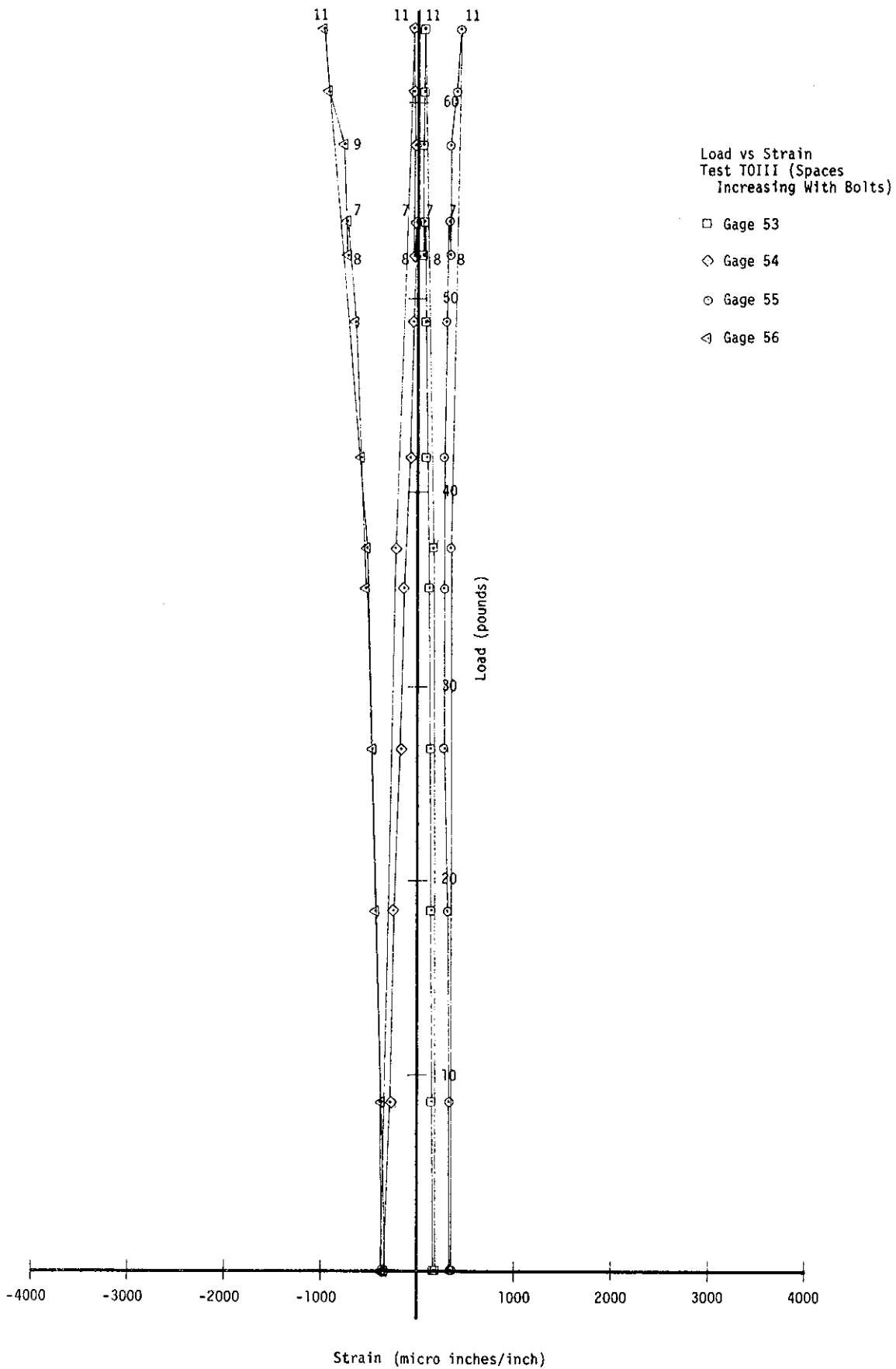
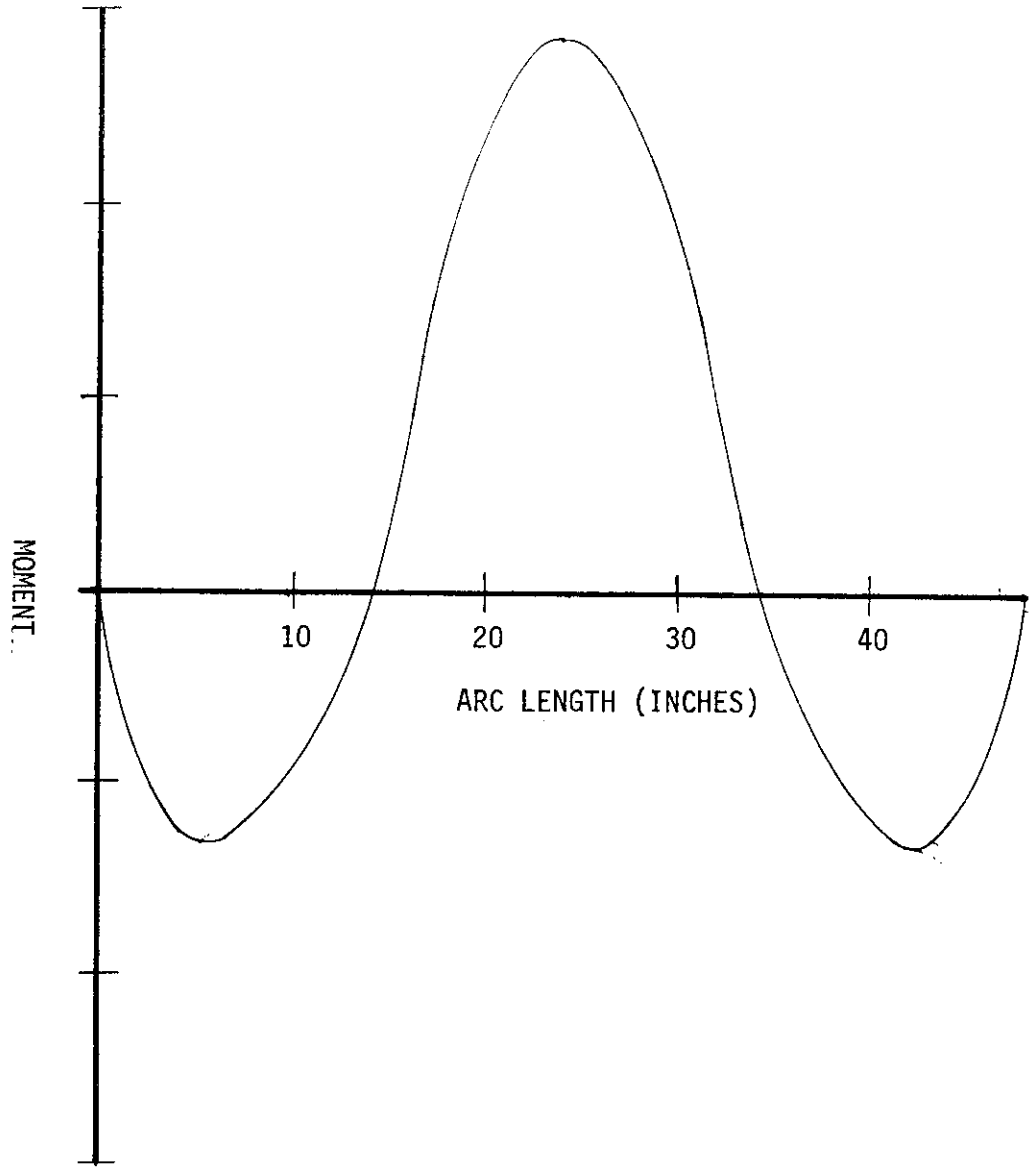


Figure 35



Moment Versus Arc Length
For a Unit Deflection

Figure 36

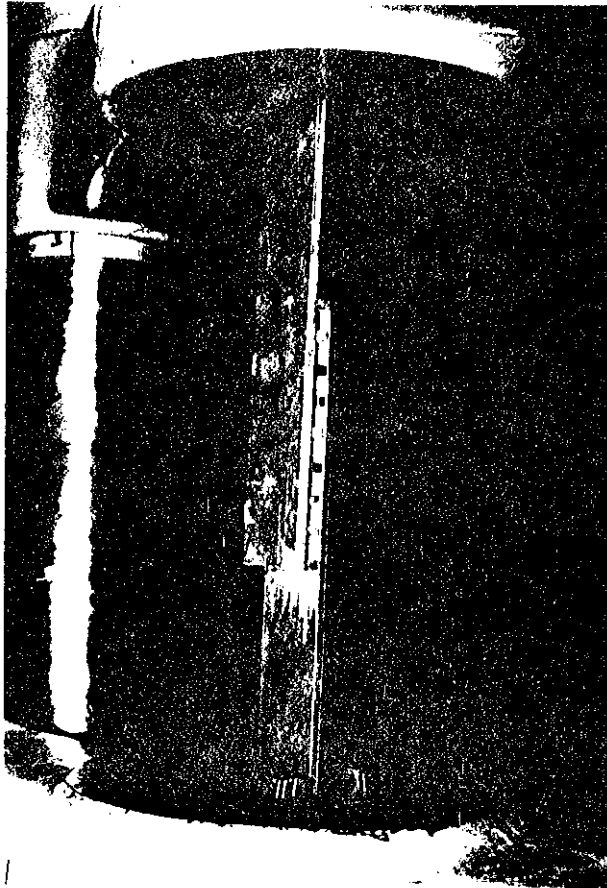
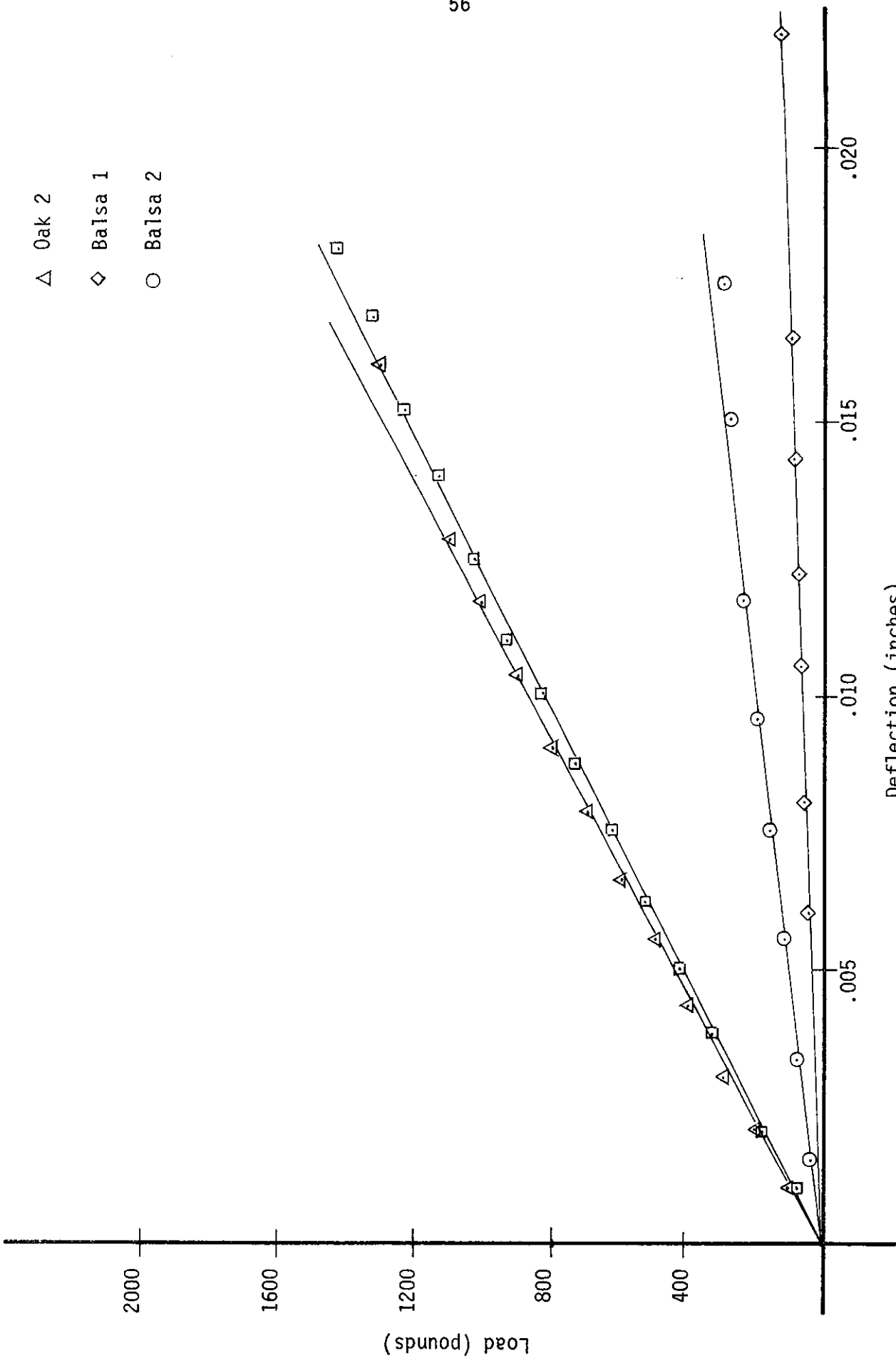


Figure 37

- Oak 1
- △ Oak 2
- ◇ Balsa 1
- Balsa 2



Deflection (inches)
Figure 38

where G_c = shear modulus of the core

τ = shear stress

λ = shear strain.

After obtaining this value, the effective shear modulus of the specimen can be obtained using another ASTM equation (4);

$$G = G_c (h) / (c + (h-c) G_c / G_f)$$

where G = effective shear modulus

h = height of sample

c = core thickness

G_f = shear modulus of the facing

It can be noted that there is not a very large difference between the effective shear modulus and the shear modulus of the core. In many cases this difference is so small that the shear modulus of the core can be substituted for the effective shear modulus. Table 2 gives ultimate shear strengths as well as the shear modulus of the core and the effective shear modulus of the specimen.

Shear Results

Shear Test Number	* V (psi)	Average V (psi)	** G _c (psi)	Average G _c (psi)	*** G (psi)	Average G (psi)
Balsa 1	123.0	219.0	396.88	1103.9	439.21	1,221.61
Balsa 2	315.0		1811.80		2004.96	
Oak 1	1468.0	1386.5	8333.40	8123.7	9220.19	8,988.23
Oak 2	1305.0		7914.00		8756.26	

*V = Ultimate Shear Strength
 **G_c = Shear Modulus of Core
 ***G = Effective Shear Modulus

Table 2

5. EVALUATION OF TEST RESULTS

5.1 Arch results

Peak load versus center displacements for all five tests are plotted in Figure 39 to show the relative increases in the load carrying capacities of each test specimen. In this plot it can be seen that the specimen with no core, TP I, behaved with extreme flexibility, achieving its peak load only after the crown of the arch had deflected 5.75 inches downward. Of the tests with cores, the balsa wood core exhibited a very stiff behavior after load point three, displacing only .1 inches in eight pounds of load. Conversely, test T0 I exhibited a much more flexible behavior, allowing for a .5 inch increase over that of the balsa in the same increment of load.

The load the balsa wood core achieved was the lowest of any of those cores tested, reaching only 24.66 pounds. This, however, still represented a 616% increase in load capacity over TP I. The load achieved by T0 I was not significantly greater than that achieved in TB I, with an increase of only 2.29 pounds. However this does represent a substantial increase when it is noted that the spacing used for the core in T0 I was three times larger than that used in TB I. In T0 I a 675% increase in load capacity was realized over TP I. The linear spacing in test T0 II removed the instabilities which developed in T0 I and led to a substantial increase in its load carrying capabilities, 45.61 pounds, for a 1137% increase over TP I. The failure in T0 II was a bond failure indicating that a larger load could be carried if a better bond between the core and the facings was developed. To this end, in the final test performed, T0 III, the same spacing was used as in T0 II, but to insure that there was no bond failure, the oak was bolted to the facings. This resulted in a local buckling failure near the north

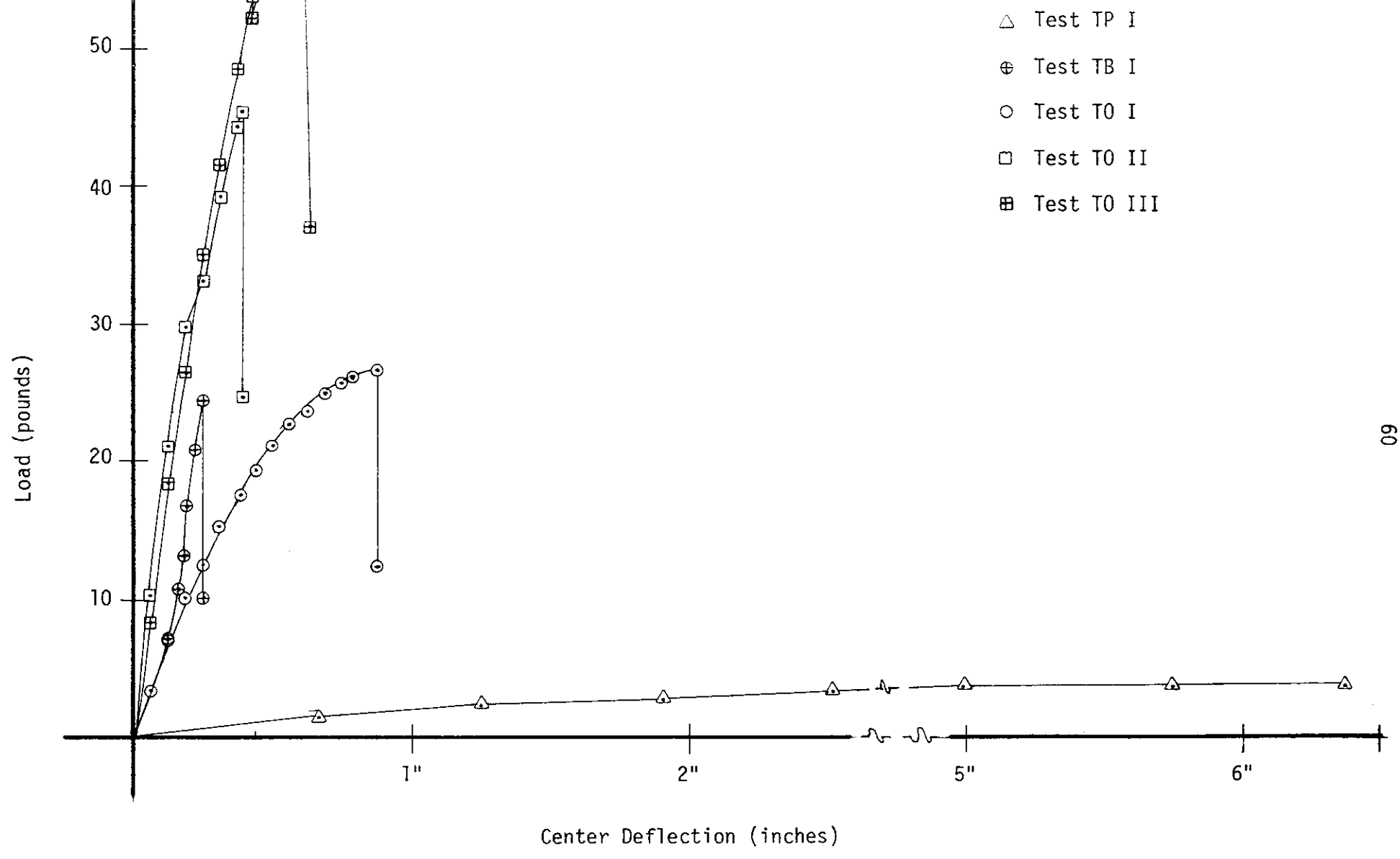


Figure 39

support. Before this buckling occurred, the load carried (63.74 pounds) was approximately 1575% greater than that of TP I. A summary of the percentage increases is presented in Table 3.

Also shown in Table 3 are the strength to weight ratios for each test. From the values tabulated on this table, the benefits of sandwich construction can easily be seen. Comparing test TP I and T0 III shows that for a 67% increase in weight, an increase of 909% in the strength to weight ratio is obtained.

5.2 Shear Test Results

Upon reviewing the shear test results for the four sandwich arches shown in Table 2, it can be seen that the modulus of shear of the specimen has a significant effect on the load carrying capacity of the arch. T0 I was able to carry a slightly greater load than TB I even though the sections of its core were spaced three times as far apart. For T0 III where linear spacing was used with bolts connecting the core to the facing, the facing of the arch buckled indicating that if the same spacing used in TB I were used with an oak core with bolts, it would be capable of attaining a load even larger than the 63.74 pounds reached in T0 III.

Summary of Arch Tests

Test	Weight (pounds)	Ultimate Load(pounds)	% Increase over TPI	Strength/Weight Ratio
TPI	.576	3.986	0	6.920
TBI	.740	24.660	616	33.320
TOI	.754	26.950	675	35.740
TOII	.856	45.61	1137	53.283
TOIII	.967	63.74	1575	62.915

Table 3

6. SUMMARY AND CONCLUSIONS

Five prebuckled arches, four sandwich and one plain, were constructed for testing in the laboratory. The plain arch was used as a basis on which to compare the remaining four sandwich arches. All four of the sandwich prebuckled arches had discrete cores with the spacing, type of wood used and any special techniques used in construction shown in Table 1. These arches were then tested to determine maximum load carrying capacity, failure mode and strains at various locations along the legs of the arch.

To facilitate the testing of the arches, a testing platform and loading mechanism were constructed and mounted on an existing frame in the laboratory. The platform was constructed such that the crown of the arch could be taken below the level of the platform. The loading mechanism was capable of applying a uniform line load across the crown of the arch, while also fixing the crown of the arch against translation. This setup performed well in all of the tests performed.

Shear tests were performed on the two types of wood cores used. From the results of these tests, the shear modulus of the core and of the overall sandwich panel was determined. These values were then used in comparing the load carrying capacity of the arches. (see section 5.2).

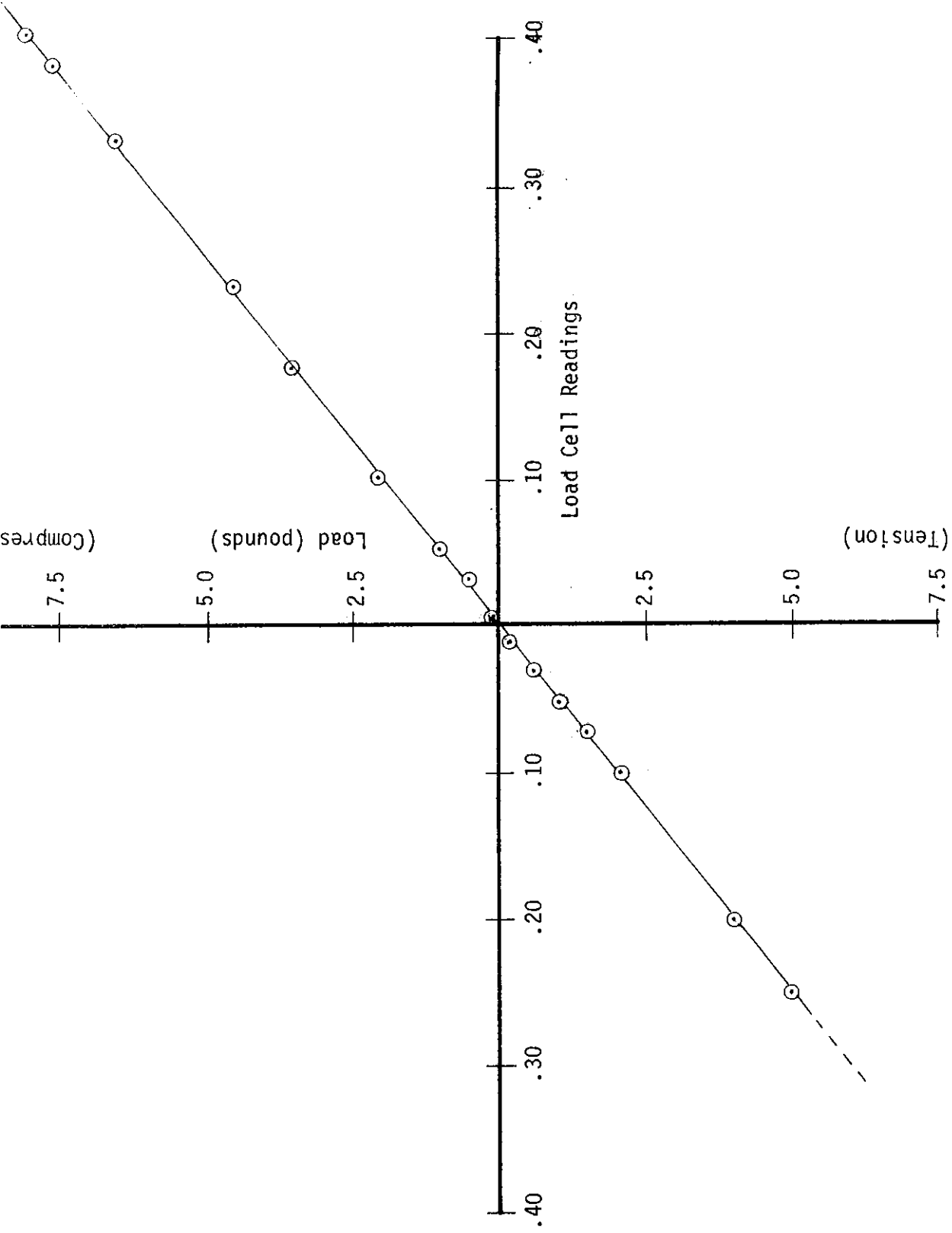
Results of the tests performed are evaluated in section 5.1. These results of tests on the prebuckled sandwich arch show that significant increases in strength to weight ratios were realized. These results combined with the relative ease with which the structure is capable of being assembled would indicate that this type of structural system would perform very well as the skeletal system for the prebuckled dome. More work needs to be done analytically to determine optimum spacing of the blocks of wood used for the

core of the arch. This however was beyond the scope of this project, but could be used as a basis for future work.

7. REFERENCES

1. Wolde Tinsae, A.M., and Huddleston, J.V., "Three Dimensional Stability Of Prestressed Arches." Journal of the Engineering Mechanics Division, ASCE, Vol.103, No. EM5, Proc. Paper 13281, October, 1977.
2. Wolde Tinsae, A.M., and Huddleston, J.V., "Non-Linear Analysis Of Self Erecting Domes." Proceedings of the Seventh Canadian Congress of Applied Mechanics, Sherbrooke, May 27-June 1, 1979.
3. Kennedy, J.S., and Aggarwal, A.S. "Effect Of Weight On Large Deflections Of Arches." Journal of the Engineering Mechanics Division, ASCE, Vol. 97, No. EM 3, June, 1971.
4. American Society For Testing And Materials, "Standard Method of Shear Test In Flatwise Plane Of Flat Sandwich Constructions Or Sandwich Cores." C 273, ASTM, 1970.
5. Allen, H.G., Analysis And Design Of Structural Sandwich Panels. New York: Pergamon Press, 1969.
6. Dietz, A.G.H., Composite Engineering Laminates. Cambridge, Massachusetts: MIT Press, 1969.
7. Kinney, J.S., Indeterminate Structural Analysis. Reading, Massachusetts: Addison-Wesley Publishing Company, Inc., 1957.
8. Platema, F.J., Sandwich Construction. New York: John Wiley and Sons, Inc., 1966.
9. Sullins, R.T., Smith, G.W., and Spier, E.E., "Manual For Structural Stability Analysis Of Sandwich Plates and Shells:" NASA CR-1457, National Aeronautics and Space Administration, Washington, D.C., December, 1969.
10. U.S. Department of Defense, Structural Sandwich Composites. Washington, D.C.: Department of Defense, 1968.

APPENDIX A
Load Cell Calibration Curve



Load Cell Calibration Curve

APPENDIX B
Tabulation Of Data

.040" Thick Arch No Core
Gage 59

Load Point	Gage 59	Load lb	Center	Comments
Buckled	0	0		
0	0	0		
.1	- .105	0		
2	- .153	0		
				Load removed and test restarted
0	.000	0	11.875	
1	- .077	-1.520	11.218	
2	- .121	- 2.390	10.625	
3	- .150	- 2.960	9.970	
4	- .169	- 3.334	9.344	LP-4. Symmetric holding.
5	- .181	- 3.571	8.740	
6	- .191	- 3.770	8.094	
7	- .197	- 3.887	7.500	
8	- .201	- 3.970	6.880	
9	- .202	- 3.986	6.125	LP-9. Load Peaked
10	- .201	- 3.970	5.500	

Test TP1 (.040" Thick Arch No Core)
(Load Cell)

.040" Thick Arch No Core (continued)
Gage 59

Load Point	Gage 59	Load lb	Center	Comments
11	- .198	- 3.907	4.875	
12	- .195	- 3.850	4.250	
13	- .188	- 3.710	3.625	
14	- .182	- 3.590	3.000	
15	- .159	- 3.140	1.750	
16	- .119	- 2.347	- .125	
17	- .060	- 1.181	- 2.000	
18	.011	+ .220	- 3.875	
19	.039	+ .773	- 4.500	LP-19. Load approximately 0.
20	.101	+1.998	- 5.750	
21	.095	+1.880	- 6.440	LP-21. Leg 100 snapped.
22	.104	+2.057	- 8.313	
23	.113	+2.235	-10.188	
24	.133	+2.630	-11.188	
25	.042	.833	-11.625	
Release	- .037			

Test TP1 (.040" Thick Arch No Core)
(Load Cell)

Strains (.040" Thick Arch No Core)(continued)
(Leg 100)

gage load point	50	51	52	53	54	55		
11	1.109	- 1.227	2.430	- 2.562	- 2.019	1.923		
12	1.171	- 1.288	2.481	- 2.611	- 2.182	2.096		
13	1.222	- 1.336	2.532	- 2.659	- 2.339	2.264		
14	1.257	- 1.370	2.545	- 2.671	- 2.485	2.424		
15	1.344	- 1.451	2.598	- 2.720	- 2.764	2.708		
16	1.450	- 1.552	2.607	- 2.727	- 3.088	3.051		
17	1.524	- 1.623	2.504	- 2.628	- 3.340	3.312		
18	1.557	- 1.656	2.400	- 2.526	- 3.407	3.385		
19	1.538	- 1.637	2.371	- 2.498	- 3.367	3.347		
20	1.421	- 1.527	2.324	- 2.450	- 3.093	3.045		
21	1.125	- 1.260	2.319	- 2.471	- 2.352	2.195		
22	1.076	- 1.213	1.942	- 2.106	- 2.344	2.230		
23	.992	- 1.135	1.366	- 1.536	- 2.251	2.182		
24	.473	- .609	- 1.472	1.424	- .673	.603		
25	.273	- .371	- 1.158	1.096	- 1.147	1.055		
Release	.358	2.489	- .804	.743	- 1.584	--		

Test TPI (.040" Thick Arch No Core)
(Leg 100)

Strains (.040" Thick Arch No Core)
(Leg 100)

gage load point	50	51	52	53	54	55		
uckled	+ .146	- .173	.697	- .831	1.171	- 1.222		
0	+ .149	- .177	.709	- .844	1.159	- 1.209		
1	.272	- .336	1.042	- 1.198	.565	- .598		
2	.368	- .452	1.277	- 1.440	.193	- .200		
0	.191	- .233	.860	- 1.001	1.055	- 1.139		
1	.294	- .362	1.132	- 1.285	.590	- .627		
2	.398	- .488	1.354	- 1.510	.218	- .231		
3	.492	- .595	1.549	- 1.702	.103	.099		
4	.582	- .692	1.718	- 1.871	.404	.383		
5	.669	- .786	1.856	- 2.006	.682	.631		
6	.747	- .869	1.987	- 2.135	.939	.861		
7	.816	- .938	2.099	- 2.244	1.177	1.085		
8	.890	- 1.013	2.195	- 2.340	1.401	1.302		
9	.969	- 1.091	2.299	- 2.441	1.649	1.547		
10	1.048	- 1.168	2.371	- 2.508	1.839	1.739		

Test TP1 (.040" Thick Arch No Core)
(Leg 100)

Deflections (.040" Thick Arch No Core)
(Leg 200)

Target load point	201	202	203	204	205	206	207	
0	2.820		6.950		10.020		11.625	
1								
2	3.129		7.390		9.890		11.187	
3								
4	3.254		7.570		9.520		9.440	
5								
6	3.473		7.540		8.960		8.280	
7								
8	3.380		7.450		8.330		7.130	
9								
10	3.440		7.390		7.640		5.875	
11								
12	3.380		7.137		6.830		4.660	
13								
14	3.380		6.890		6.020		3.500	
15								

Test TP1 (.040" Thick Arch No Core)
(Leg 200)

Strains (Balsa Core Spaced @ 5/8" O.C.) (continued)
Gage 59

Load Point	Gage 59	Load lb	Center	Comments
13	- .789	-15.580	11.188"	LP-16. More wood separates from skin 7, 9, 10, 11, 13, 14, 16 (top skin) 8, 9, 10 (lower skin). Reading on 59 reached 1.2 before big snap.
14	- .872	-17.215	11.063"	
15	- .970	-19.150	10.875"	
16	- .781	-15.420	10.625"	
17	- .216	-4.26	10.315"	
18				

Test B1 (Balsa Core Spaced @ 5/8" O.C.)
(Load Cell)

Strains (Balsa Core Spaced @ 5/8" O.C.)
(Leg 100)

gage Load Point	40	41	42	43	44	45		
TB BF	.254	.772	.581	.485	.298	.119		
T & B B	.117	.486	.705	.641	.496	.082		
Glued	.283	.501	.874	.637	.600	.333		
0	0	0	0	0	0	0		
1	.005		- .045	.057	.013	- .011		
2	.006		- .075	.098	.023	- .002		
3	.006		- .109	.116	.023	- .025		
4	.006		- .172	.153	.026	- .032		
4 on	.001		- .190	.157	.026	- .034		
4 off	- .001		- .186	.146	.025	- .033		
5	.002		- .217	.208	.039	- .045		
6	- .001		- .335	.271	.039	- .055		
7	- .005		- 1.839	.160	.024	- .044		
8	- .006		- 2.339	.243	- .018	- .027		
9	- .003		- 2.361	.209	.049	- .051		

Test B1 (Balsa Core Spaced @ 5/8" O.C.)
(Leg 100)

Strains (Balsa Core Spaced @ 5/8" O.C.) (continued)
(Leg 100)

gage load point	40	41	42	43	44	45		
10	- .002		- 2.466	.249	.069	- .061		
11a	0		- 2.679	.255	.070	- .063		
11b	- .003		- 1.539	.245	.069	- .065		
12	0		- 1.958	.313	.098	- .079		
13	0		- 2.318	.371	.121	- .107		
14	- .001		- 2.563	.419	.139	- .134		
15	.002		- 2.980	.522	.181	- .211		
16	.002		- 1.853	.655	.208	- .329		
17	.006		- 2.290	.139	.009	- .085		

Test B1 (Balsa Core Spaced @ 5/8" O.C.)
(Leg 100)

Strains (Balsa Core Spaced @ 5/8" O.C.)
(Leg 200)

gage load point	46	47	48	49				
TB BF	.002	.001	0	-.753				
T & B B	-.082	-.445	-.643	-.470				
Glued	-.045	-.470	-.597	-.385				
0	0	0	0	0				
1	-.087	-.037	.036	.035				
2	-.145	-.067	.065	.064				
3	-.160	-.068	.075	.069				
4	-.197	-.076	.085	.076				
4 on	-.192	-.074	.097	.085				
4 off	-.180	-.067	.091	.079				
5	-.250	-.108	.129	.115				
6	-.291	-.110	.142	.125				
7	-.173	-.069	.091	.088				
8	-.211	-.105	.119	.091				
9	-.235	-.117	.124	.127				

Test B1 (Balsa Core Spaced @ 5/8" O.C.)
(Leg 200)

Strains (Balsa Core Spaced @ 5/8" O.C.) (continued)
(Leg 200)

gage load point	46	47	48	49				
10	- .288	- .157	.153	.154				
11a	- .294	- .161	.158	.159				
11b	- .285	- .164	.157	.159				
12	- .372	- .227	.204	.206				
13	- .442	- .282	.247	.248				
14	- .497	- .326	.286	.278				
15	- .603	- .410	.377	.333				
16	- .706	- .458	.468	.364				
17	- .023	- .012	.056	.043				

Test B1 (Balsa Core Spaced @ 5/8" O.C.)
(Leg 200)

Oak Core Spaced @ 1-7/8" O.C.
Gage 59

Load Point	Gage 59	Load lb	Center inches	
1	-.181	-3.571	11.938	LP-0 Curve not completely smooth possibly due to curing
2	-.362	-7.145	11.875	
3	-.519	-10.24	11.813	LP-3 Symmetric behavior
4	-.650	-12.83	11.750	
5	-.778	-15.36	11.688	
6	-.902	-17.81	11.625	LP-6 South side slightly higher, some instability between blocks. More noticeable in top face
7	-.983	-19.41	11.563	
8	-1.075	-21.22	11.50	
9	-1.161	-22.92	11.438	LP-9 Instability in first 3 spans either side of crown.
10	-1.212	-23.93	11.375	LP-10 Slight instability in 4th large span.
11	-1.271	-25.09	11.313	
12	-1.315	-25.96	11.250	
13	-1.399	-26.44	11.219	
14	-1.361	-26.87	11.125	
15	-1.365	-26.95	11.063	
16	-.639	-12.61	11.063	LP-16 Failure in oak piece #3 south displaced approx. 1/4" south relative to bottom Instab. gone

Oak Core Spaced @ 1-7/8" O.C.
(Load Cell)

Oak Core Spaced @ 1-7/8" O.C. (continued)
Gage 59

Load Point	Gage 59	Load lb	Center inches	
17	-.648	-12.80	11.00	LP-17. 7th large span north side, bottom skin buckling
18	-.704	-13.90	10.875	
19	-.728	-14.37	10.750	
20	-.723	-14.27	10.625	
21	-.703	-13.881	10.50	
22	-.673	-13.30	10.375	LP-22 Arch would move sideways if not restrained. Buckling at span 7 becoming more severe

Oak Core Spaced at 1-7/8" O.C.
(Load Cell)

Oak Core Spaced @ 1-7/8" O.C.
Gage 59

Load Point	Gage 59	Load lb	Center	Comments
23	- .662	- 13.070	10.313	
24	- .638	- 12.590	10.063	
25	- .363	- 7.165	9.813	
26	- .403	- 7.954	9.563	
27	- .417	- 8.231	9.313	
28	- .315	- 6.217	9.313	LP-28 5th South piece snapped
29	- .332	- 6.550	9.063	
30	- .352	- 6.950	8.688	
31	- .372	- 7.340	8.313	
32	- .390	- 7.698	7.938	
33	- .400	- 7.895	7.563	
34	- .305	- 6.020	7.188	LP-34. Load dropped shifted to north slightly.
35	- .296	- 5.842	6.813	LP-35. At Span 7 bottom skin touching top skin.
36	- .312	- 6.160	6.688	
37	- .298	- 5.880	6.375	
38	- .284	- 5.605	6.000	

Oak Core Spaced @ 1-7/8" O.C.
(Load Cell)

Oak Core Spaced @ 1-7/8" O.C. (continued)
Gage 59

Load Point	Gage 59	Load lb	Center	Comments
39	- .271	- 5.350	5.625	
40	- .261	- 5.150	5.125	
41	- .244	- 4.815	4.625	
42	- .224	- 4.420	4.250	
43	- .206	- 4.064	3.563	
44	- .085	- 1.675	.938	LP-44. Top even with table top.
45				LP-45. Load approximately 0.
46	.017	.339	- 1.563	
47	.040	.793	- 2.188	LP-47. Tension in load cell.
Release	.123	2.430	0	After release arch rebounded to near original position with permanent deformation.

Test T01 (Oak Core Spaced @ 1-7/8" O.C.)
(Load Cell)

Strains (Oak Core Spaced @1-7/8" O.C.)
(Leg 100)

Gage Load Point	40	41	42	43	44	45		
Flat	0.0	0.0	0.0	0.0	0.0	0.0		
BB&TF	.127	-.081	-.005	-.593	-.124	-.565		
TB&BB	XXXX	-.072	.381	-.639	.551	-.517		
1	.009	-.057	-.028	.134	-.161	.138		
2	-.021	-.092	.05	.234	-.469	.241		
3	-.037	-.126	.079	.365	-.726	.336		
4	-.059	-.152	.128	.467	-1.019	.416		
5	-.077	-.185	.158	.618	-1.324	.491		
6	-.105	-.215	.213	.731	-1.683	.553		
7	-.120	-.235	.236	.884	-1.959	.613		
8	-.134	-.269	.262	1.067	-2.261	.664		
9	-.170	-.299	.313	1.190	-2.708	.705		
10	-.172	-.309	.331	1.426	-2.927	.750		
11	-.206	-.338	.373	1.568	-3.376	.781		
12	-.203	-.360	.378	1.937	-3.602	.811		

Test T0 I (Oak Core Spaced @ 1-7/8" O.C.)

(Leg 100)

Strains (Oak Core Spaced @ 1-7/8" O.C.)
(Leg 100)

gage point	40	41	42	43	44	45		
23	- .209	- .160	.490	6.236	- 7.822	.611		
24	- .221	- .139	.511	6.848	- 8.013	.640		
25	- .129	- .103	.353	6.653	- 5.861	.481		
26	- .144	- .121	.379	6.883	- 6.262	.570		
27	- .152	- .120	.393	7.153	- 6.560	.626		
28	- .111	- .100	.315	7.021	- 5.339	.558		
29	- .116	- .103	.323	7.242	- 5.627	.619		
30	- .122	- .106	.337	7.643	- 6.028	.700		
31	- .128	- .107	.349	7.936	- 6.423	.778		
32	- .134	- .112	.362	8.234	- 6.804	.839		
33	- .141	- .111	.371	8.454	- 7.120	.893		
34	- .136	- .065	.366	8.402	- 7.388	.711		
35	- .136	- .058	.362	8.479	- 7.580	.728		
36	- .055	- .073	.369	8.522	- 7.679	.972		
37	- .053	- .060	.368	8.595	- 7.881	.972		
38	- .052	- .063	.371	8.652	- 8.059	.960		

Test T01 (Oak Core Spaced @ 1-7/8" O.C.)
(Leg 100)

Strains (Oak Core Spaced @ 1-7/8" O.C.) (continued)
(Leg 200)

Gage Location	46	47	49	50	51	52		
Flat	0.0	0.0	0.0	0.0	0.0	0.0		
BB&TF	-.138	-.439	-.199	-.001	-.177	.037		
BB&TB	.582	-.429	-.182	-.001	-.159	-.238		
1	-.026	.164	.029	-.001	-.001	-.014		
2	-.043	.318	.074	0.000	-.004	.017		
3	-.050	.440	.109	-.001	-.005	.026		
4	-.057	.555	.151	-.001	-.004	.046		
5	-.053	.661	.188	0.000	-.006	.059		
6	-.052	.758	.229	-.002	-.005	.083		
7	-.034	.848	.270	-.001	-.002	.097		
8	-.023	.925	.300	-.002	-.002	.108		
9	.005	1.016	.356	-.002	.002	.139		
10	.024	1.087	.386	-.001	.002	.139		
11	.050	1.169	.446	-.002	.001	.175		
12	.075	1.223	.457	-.001	-.004	.176		

Test TO I (Oak Core Spaced @ 1-7/8" O.C.)
(Leg 200)

Strains (Oak Core Spaced @ 1-7/8" O.C.)
(Leg 200)

gage load point	46	47	49	50	51	52		
23	- .062	4.033	.368	.001	.021	.236		
24	- .045	4.244	.387	.001	.024	.248		
25	- .054	4.004	.200	0	.027	.159		
26	- .049	4.443	.218	.001	.031	.174		
27	- .037	4.767	.230	.001	.033	.183		
28	- .049	3.980	.172	0	.029	.144		
29	- .037	4.278	.181	.001	.031	.149		
30	- .003	4.671	.191	- .002	.033	.155		
31	.055	5.032	.201	- .001	.034	.161		
32	.133	5.409	.208	0	.034	.167		
33	.238	5.731	.216	0	.035	.171		
34	.022	6.015	.220	0	.034	.169		
35	.039	6.215	.224	- .004	.039	.168		
36	.078	6.302	.228	- .001	.037	.172		
37	.079	6.506	.233	- .001	.036	.170		
38	.070	6.714	.237	0	.035	.172		

Test T01 (Oak Core Spaced @ 1-7/8" O.C.)
(Leg 200)

Strains (Oak Core Spaced @ 1-7/8" O.C.) (continued)
(Leg 200)

gage Load Point	46	47	49	50	51	52		
39	.064	6.891	.240	- .001	.035	.173		
40	.076	7.110	.244	- .002	.035	.174		
41	.081	7.345	.248	- .001	.034	.175		
42	.073	7.498	.252	- .001	.034	.175		
43	.070	7.630	.251	- .001	.034	.173		
44	.040	8.224	.249	- .001	.032	.154		
45								
46	.040	8.570	.232	- .001	.026	.107		
47	.040	8.632	.224	- .002	.024	.089		
Release	.081	2.413	.138	- .002	.039	.079		

Test T01 (Oak Core Spaced @ 1-7/8" O.C.)
(Leg 200)

Spaces Increasing From Center
Gage 59

Load Point	Gage 59	Load lb	Center	Comments
0	0	0	12.250	
1	- .527	-10.426	12.188	
2	- 1.071	-21.200	12.125	
3	- 1.516	-29.999	12.063	LP-3. Cracking sound.
4	- 1.673	-33.104	12.000	LP-4. More cracking sounds. No visible signs yet. Load still increasing.
5	- 1.990	-39.380	11.938	LP-5. Some uplift noticed rod & weight not heavy enough.
6	- 2.246	-44.440	11.875	LP-6. Some glue separation noticed in 2 south piece but not all the way across piece.
6.5	- 2.305	-45.610		LP-6.5. Weight added. Load visually peaked at 2.374 before failure.
7	- 1.262	-24.970		LP-7. Failure.
Release	.107	2.120	12.250	

Test TOII (Spaces Increasing From Center)
(Load Cell)

Strains (Spaces Increasing From Center)
(Leg 100)

gage load point	40	41	42	43	44	45	46	
Flat	0	0	0	0	0	0	0	
BB TF	- .089	.003	.004	.491	- .337	.001	.006	
Glued	.809	.766	- .485	.389	.111	1.424	- .750	
0	0	0	0	0	0	0	0	
1	.235		- .146	.113	.087	- .092	- .166	
2	.468		- .289	.228	.186	- .219	- .313	
3	.677		- .412	.322	.268	- .417	- .348	
4	.826		- .507	.394	.333	- .741	- .307	
5	.913		- .571	.439	.375	- 1.377	- .035	
6	1.009		- .635	.486	.431	- 1.847	.297	
7	.589		- .255	.192	.121	- 4.032	2.950	
Release	- .029	.250	.028	- .046	0	- .493	.142	

Test TOII (Spaces Increasing From Center)
(Leg 100)

Strains (Spaces Increasing From Center)
(Leg 100)

gage ad int	47	48	49	50	51	52	53	
Flat	0	0	0	0	0	0	0	
BB TF	.463	- .401	- .001	.003	.787	- .616	.011	
Glued	.521	- .456	.693	- .427	.249	- .246	.170	
0	0	0	0	0	0	0	0	
1	.179	.062	.194	- .140	.102	- .189	.007	
2	.360	.127	.452	- .301	.195	- .422	.014	
3	.457	.281	.651	- .447	.298	- .613	.031	
4		1.191	.760	- .512	.342	- .709	.036	
5		1.531	.911	- .606	.402	- .846	.045	
6		1.778	1.060	- .699	.467	- .986	.049	
7		2.728	.552	- .222	.061	- .470	.014	
Release		.333	- .032	.050	- .027	.035	.073	

Test TOII (Spaces Increasing From Center)
(Leg 100)

Strains (Spaces Increasing From Center)
(Leg 100)

gage ad int	54	55	56					
Flat	0	0	0					
BB TF	.002	.326	- .302					
Glued	.116	.336	- .356					
0	0	0	0					
1	.057	- .015	- .015					
2	.136	- .026	- .075					
3	.187	- .025	- .132					
4	.219	- .026	- .153					
5	.258	- .035	- .182					
6	.298	- .033	- .210					
7	.210	- .034	- .089					
Release	.004	.006	.089					

Test TOII (Spaces Increasing From Center)
(Leg 100)

Spaces Increasing From Center
Gage 59

Load Point	Gage 59	Load lb	Center	Comments
0	0	0	12.375	
1	- .438	- 8.650	12.313	
2	- .935	- 18.500	12.250	
3	- 1.359	- 26.830	12.188	
4	- 1.777	- 35.090	12.125	LP-4. No changes yet.
5	- 2.115	- 41.763	12.063	
6	- 2.470	- 48.773	12.000	
7	- 2.732	- 53.950	11.938	LP-7. Slight cracking sound some separation of oak from skin at 2 north location, just at edge not all the way across. Slight depression at crown.
7	- 2.642	- 52.170		
8	- 2.925	- 57.760	11.875	LP-8. 2 south some separation from bottom skin.
9	- 3.071	- 60.640	11.830	LP-9. 1 south separated from bottom skin. Local instabilities visible between oak pieces visible all the way across arch most pronounced near supports.
10	- 3.228	- 63.740	11.766	
11	- 1.877	- 37.060	11.735	LP-11. Local buckling of bottom skin at 17th span. North all instabilities dissipated.
12			12.125	LP-12. Load released permanent deformation in Span 17.
Release	.005	.102		

Test TOIII (Spaces Increasing From Center)
(Load Cell)

Strains (Spaces Increasing From Center)
(Leg 100)

gage load point	40	41	42	43	44	45	46	
Flat	0	0	0	0	0	0	0	
BB TB	- .089	.003	.004	.491	- .337	.001	.006	
Glued	.809	.766	- .485	.389	.111	1.425	- .750	
0	0	0	0	0	0	0	0	
1	.141	- .098	- .105	.099	.066	.041	- .235	
2	.345	- .210	- .225	.209	.126	.049	- .461	
3	.484	- .306	- .338	.306	.204	.094	- .699	
4	.677	- .407	- .465	.411	.272	.107	- .926	
5	.799	- .487	- .579	.496	.352	.164	- 1.160	
6	.985	- .579	- .713	.589	.423	.299	- 1.464	
7	1.104	- .648	- .834	.669	.501	.440	- 1.762	
7.5	1.051	- .694	- .841	.681	.496	.492	- 1.739	
8	1.236	- .779	- .999	.788	.557	.510	- 1.939	
9	1.279	- .822	- 1.097	.839	.612	.639	- 2.139	
10	1.429	- .971	- 1.190	.871	.714	.863	- 2.464	

Test TOIII (Spaces Increasing From Center)
(Leg 100)

Strains (Spaces Increasing From Center)
(Leg 100)

gage load point	48	49	50	51	52	53	54	
Flat	0	0	0	0	0	0	0	
BB TF	- .401	- .001	.003	.787	- .616	.011	.002	
Glued	- .456	.693	- .427	.249	- .246	.170	- .356	
0	0	0	0	0	0	0	0	
1	- .027	.193	- .100	.0450	- .168	- .019	.065	
2	- .031	.374	- .232	.138	- .340	- .031	.111	
3	- .064	.586	- .351	.202	- .536	- .047	.178	
4	- .050	.762	- .487	.309	- .715	- .059	.219	
5	- .043	.967	- .615	.386	- .903	- .071	.271	
6	- .089	1.135	- .750	.496	- 1.069	- .083	.305	
7	- .116	1.330	- .883	.589	- 1.261	- .098	.350	
7.5	- .107	1.279	- .841	.553	- 1.205	- .109	.316	
8	- .065	1.421	- .980	.678	- 1.360	- .116	.328	
9	.442	1.563	- 1.081	.750	- 1.496	- .093	.311	
10	.529	1.644	- 1.187	.854	- 1.588	- .094	.314	

Test TOIII (Spaces Increasing From Center)
(Leg 100)

Strains (Spaces Increasing From Center)
(Leg 100)

gage load point	55	56						
Flat	0	0						
BB TF	.326	- .302						
Glued	.336	- .356						
0	0	0						
1	- .019	- .034						
2	- .030	- .073						
3	- .039	- .126						
4	- .042	- .174						
5	- .043	- .240						
6	- .036	- .302						
7	- .015	- .395						
7.5	- .004	- .375						
8	.002	- .424						
9	.067	- .571						
10	.112	- .636						

Test TOIII (Spaces Increasing From Center)
(Leg 100)

Deflections (Spaces Increasing From Center)
(Leg 100)

Target Load Point	101	102	103	104	105	106	107	
0	3.086		7.133		10.336		11.644	
1								
2								
3								
4	3.180		7.227		10.370		12.398	
5								
6								
7	3.180		7.260		10.273		12.270	
8								
9								
10	3.180		7.290		10.211		12.160	
11	2.992		6.914		9.960		12.010	
12	3.117		7.100		10.336		12.464	

Test TOIII (Spaces Increasing From Center)
(Leg 100)

Deflections (Spaces Increasing From Center)
(Leg 200)

Target ad int	201	202	203	204	205	206	207	
0	3.070		7.080		10.230		11.600	
1								
2								
3								
4								
5								
6								
7	3.070		7.150		10.040		12.164	
8								
9								
10	3.195		7.210		10.040		12.055	
11	3.450		7.398		10.164		12.087	
12	3.195		7.150		10.290		12.383	

Test TOIII (Spaces Increasing From Center)
(Leg 200)